Quantum Materials towards Metrology

Dr. Sunil Singh Kushvaha

CSIR-National Physical Laboratory,

Dr. K.S. Krishnan Road, New Delhi-110012

5-day Symposium and workshop on "Quantum Information and Technologies (QIT)", *24-28*th July 2025, IIIT Allahabad, Prayagraj, India

Outline

- **Quantum Metrology: Towards SI Traceable Measurements**
- **Quantum Materials: Topological Insulators**
- **Quantum based characterization technique: STM**
- **Future towards Quantum Anomalous Hall Effect**
- **Conclusion and future remark**

Metrology: Basic need

Metrology: Metrology is the science of measurement. It establishes standardized units and methods that are accepted worldwide, ensuring consistency and accuracy in various fields like science, technology, and trade. By establishing a common understanding of measurements, metrology facilitates global collaboration, commerce, and technological advancement.

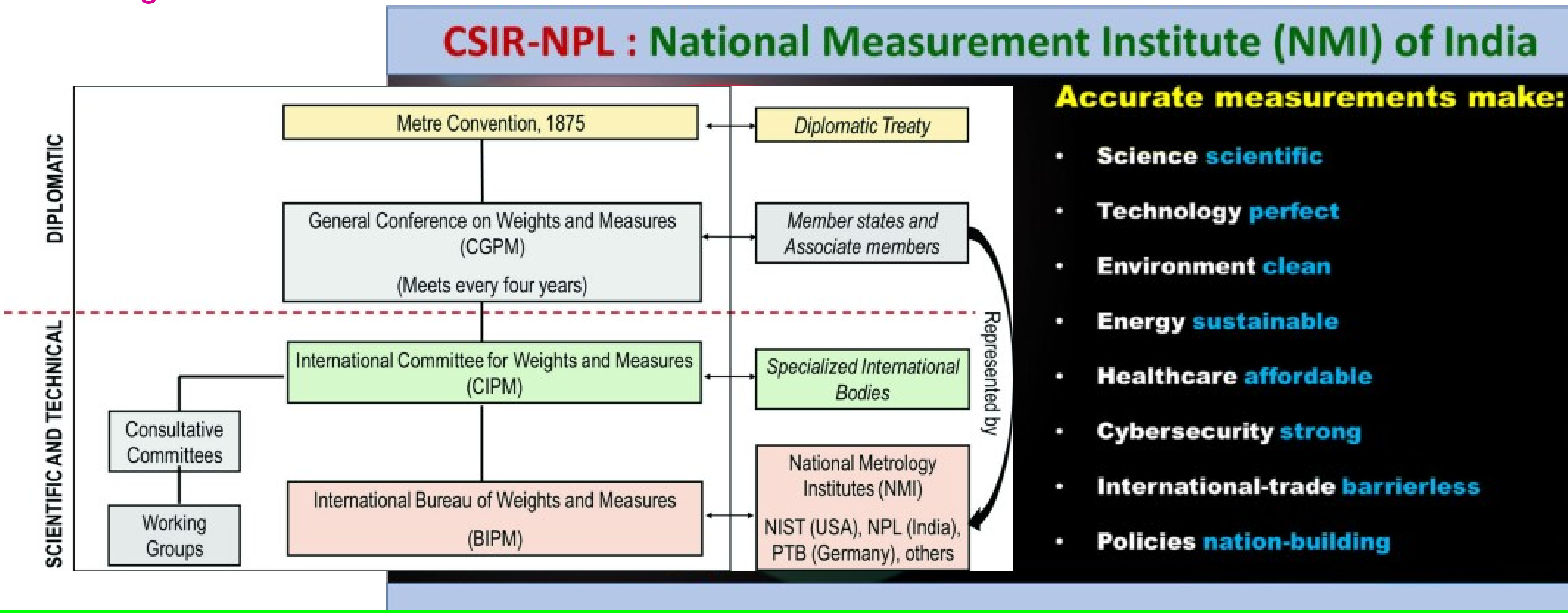

Metrology: Basic need

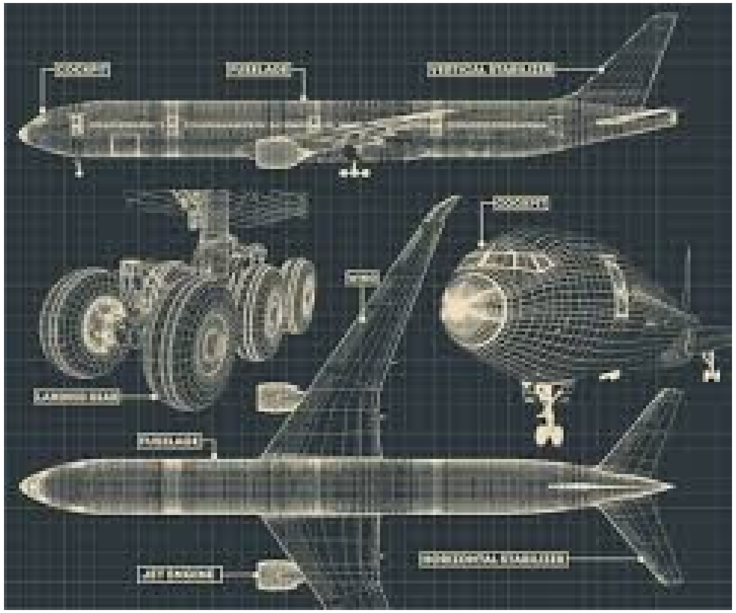

National Status of SI Units

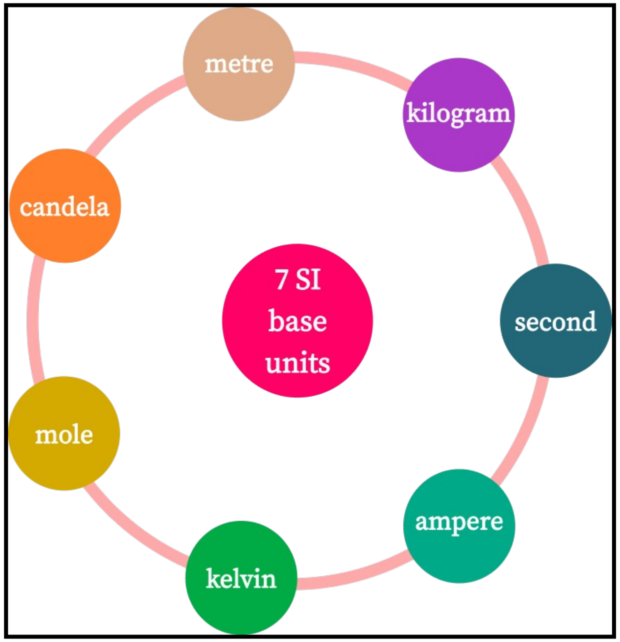

Realization of SI Units at NPLI

QUANTITY	UNITS	SYMBOL	STANDARD	UNCERTAINTY
Length	metre	m	Iodine stabilized He-Ne laser 633nm	2.1×10^{-11}
Mass	kilogram	kg	International Prototype *copy No. 57*	4.6×10^{-9}
Time	second	s	Cs Atomic clock	1×10^{-13}
Electric Current	ampere	A	Realized through voltage & resistance	1×10^{-6}
Temperature	kelvin	K	Triple point of water	1.7×10^{-4}
Luminous Intensity	candela	cd	A set of standard lamps	$(1.6 \text{ to } 1.3) \times 10^{-2}$
Amount of substance	mole	mol	Chemical route	

SI BASE UNITS and THEIR DERIVED UNITS

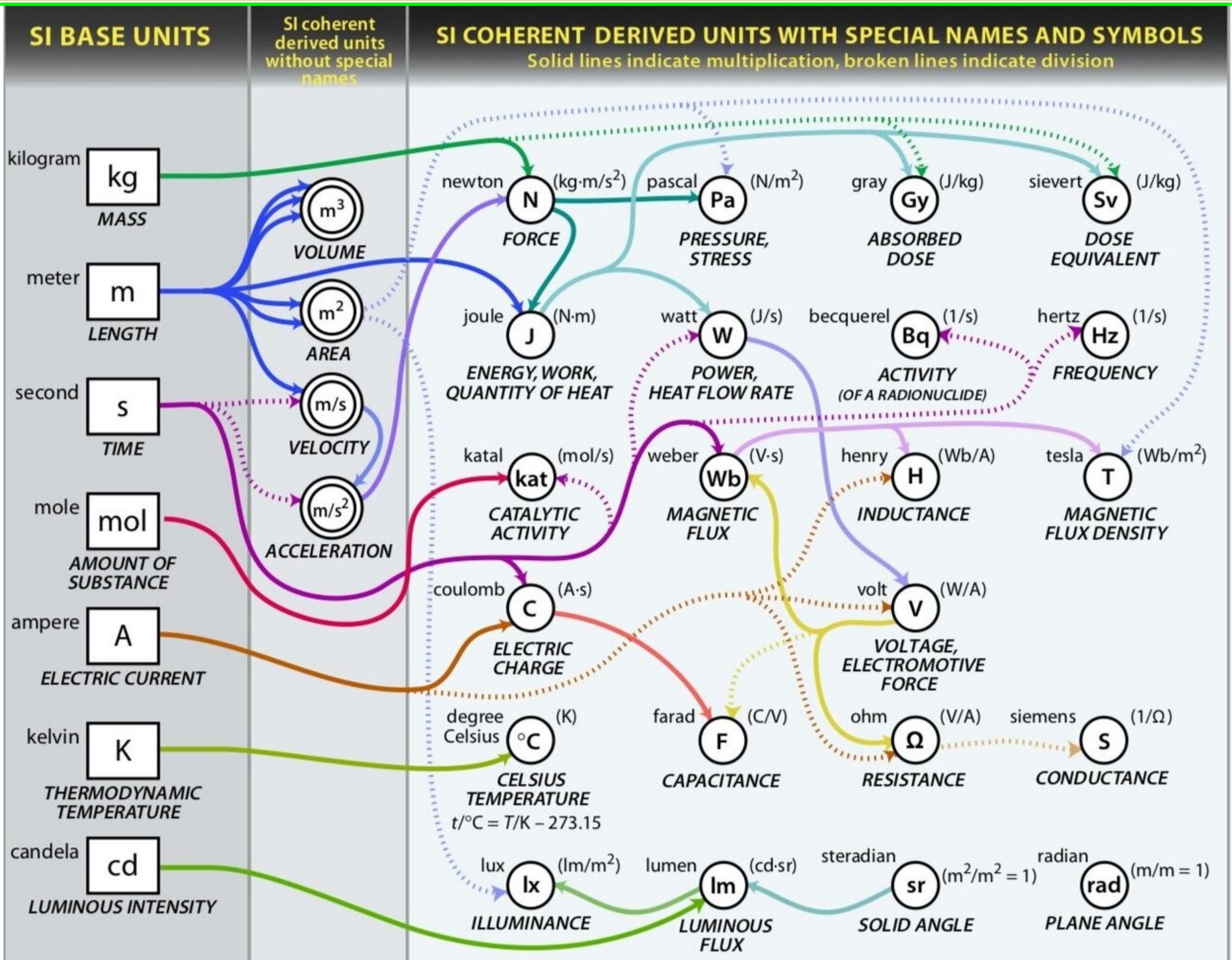

Quantum Metrology: Traceable to SI units

26th meeting of the General Conference on Weights and Measures (CGPM), means that from 20 May 2019, all SI units are defined in terms of constants that describe the natural world. This will assure the future stability of the SI and open the opportunity for the use of new technologies, including quantum technologies, to implement the definitions.

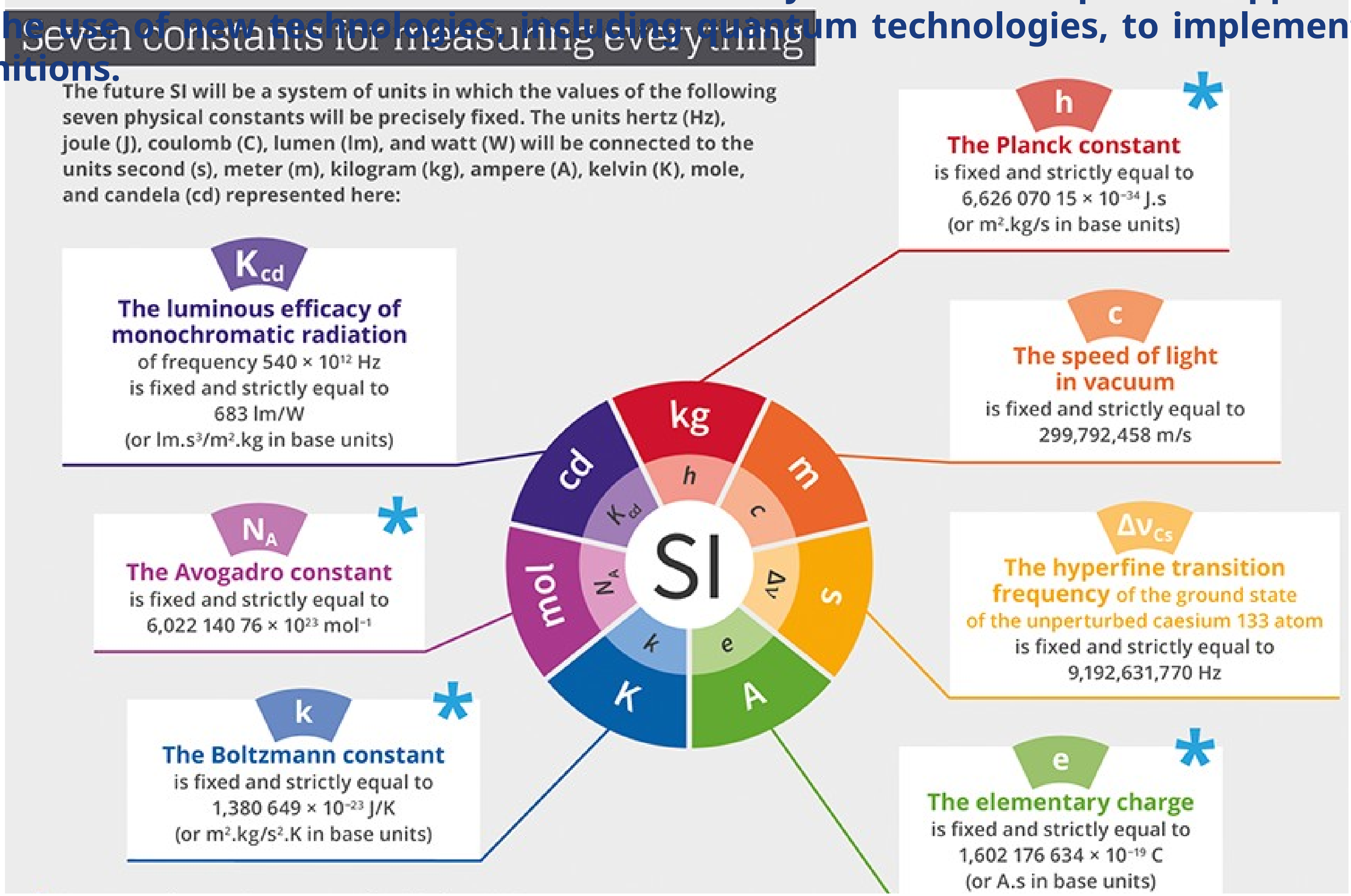

Quantum Metrology: Planck constant

Planck constant (h)-based metrology, a fundamental constant in quantum mechanics, to define and realize SI units, particularly the kilogram. The kilogram, previously defined by a physical artifact (the International Prototype of the Kilogram), is now being redefined based on a fixed numerical value of the Planck constant. This means that the Planck constant, along with other defined constants like the speed of light and the cesium frequency, will underpin the definition of Kg.

- A key instrument in this redefinition is the Kibble balance. It relates the Planck constant to a mass by balancing gravitational force with electromagnetic force.

Benefits of Planck Constant-Based Metrology:

Improved Precision: Redefining units based on fundamental constants like h eliminates the reliance on physical artifacts, leading to more precise measurements.

Greater Stability: Fundamental constants are believed to be invariant in time and space, making the redefined units more stable and reliable.

Global Consistency: A consistent definition of units based on fundamental constants ensures greater uniformity in measurements across different laboratories and countries.

Advancement of Science and Technology: Planck constant-based metrology supports advancements in various fields, including quantum computing, materials science, and fundamental physics research.

Planck Constant based Kibble Balance

The **kilogram**, symbol **kg**, is the SI unit of mass. It is defined by taking the fixed numerical value of the **Planck constant *h*** to be $6.62607015 \times 10^{-34}$ when expressed in the unit J s, which is equal to kg m^2 s^{-1}, where the metre and the second are defined in terms of c and $\Delta\nu_{Cs}$.

$$1 \text{ Kg} = \left(\frac{h}{6.626\,070\,15 \times 10^{-34}}\right) m^{-2} s$$

which is equal to:

$$1 \text{ Kg} = \frac{(299792458)^2}{(6.626\,070\,15 \times 10^{-34})(9192631770)} \frac{h\,\Delta\nu_{Cs}}{c^2} \approx 1.4755214 \times 10^{40} \frac{h\,\Delta\nu_{Cs}}{c^2}$$

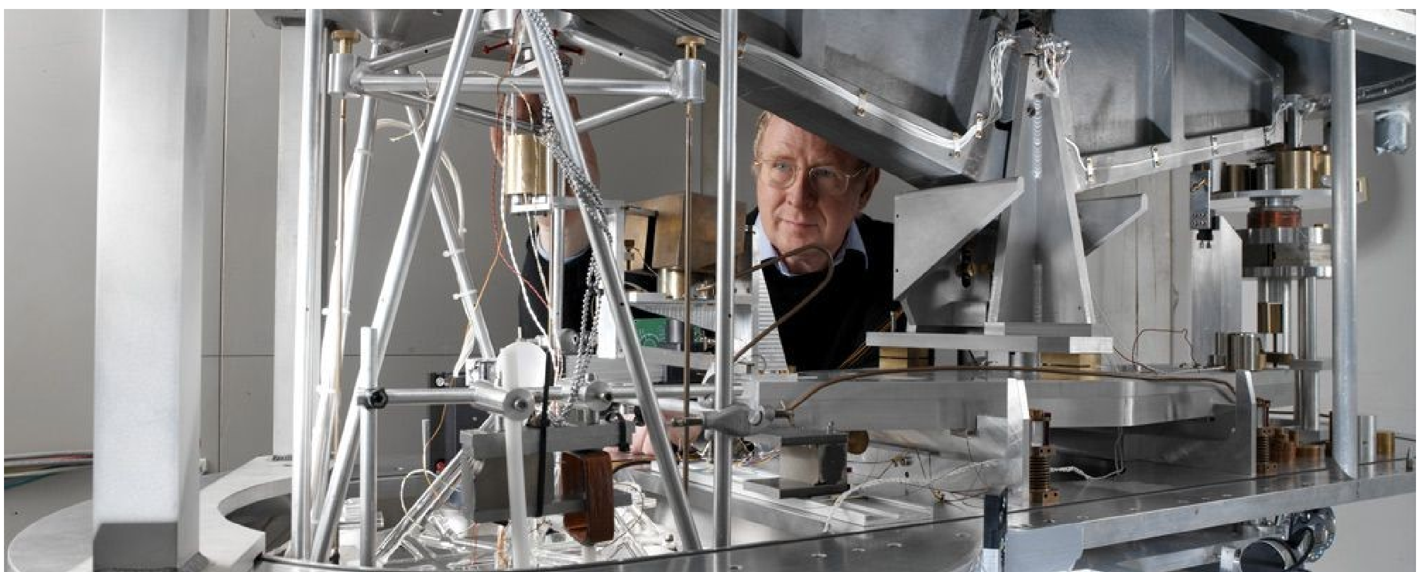

Planck Constant based Kibble Balance

STATIC MODE

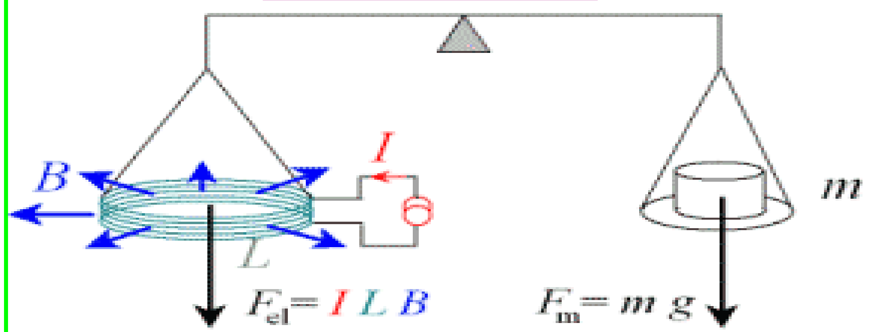

DYNAMIC MODE

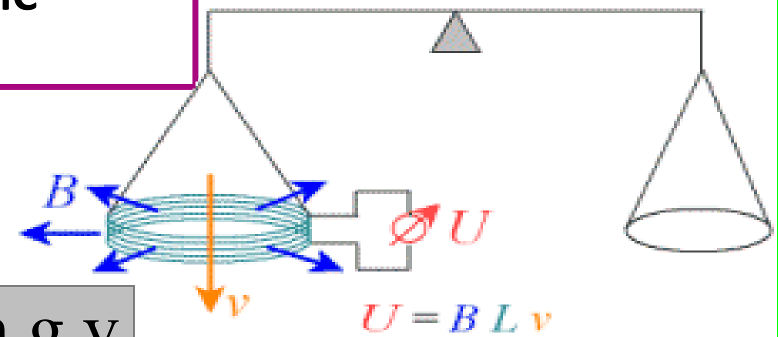

$$U.I = m.g.v$$

Introducing Quantum standards for U and I measurement

m g = I BL ……..(i)

BL= mg/I……(ii)

U = B L v ….. (iii)

BL= U/v……(iv)

$$\boldsymbol{m} = \frac{bf^2}{4gv}\boldsymbol{h}$$

f = experimental frequency
b = a dimensionless quantity originating from quantum voltage and current measurement

$$U.I = m.g.v$$

This equation essentially equates the mechanical power (right side) required to move a mass (m) at a certain velocity (v) in a gravitational field (g) to the electrical power (left side) supplied to a coil to achieve the same mechanical effect. The Kibble balance uses this principle to precisely determine mass by balancing the mechanical force exerted by a mass in a magnetic field with the electrical force produced by passing a current through a coil in the same magnetic field.

100 g: Kibble Balance

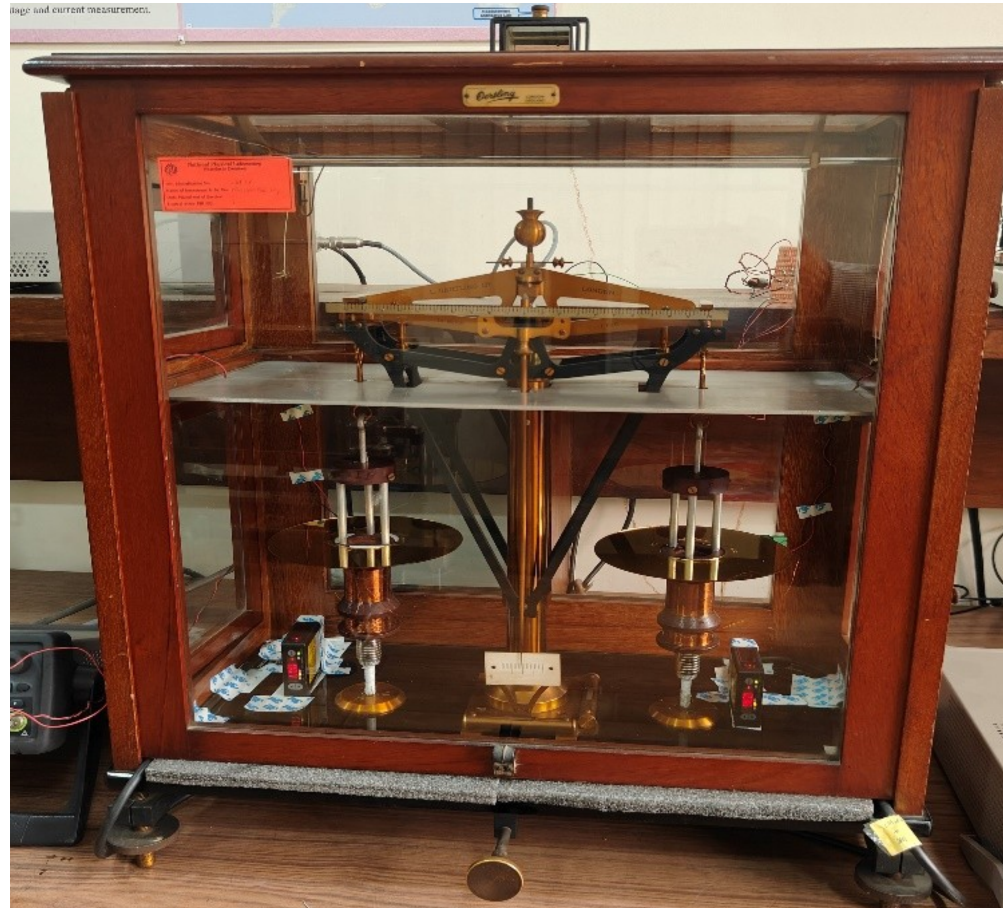

Old 1 kg Two pan Balance
Modified for 100 g Kibble balance

Courtesy: D.D. Shivagan and N. Singh

Quantum Electrical Metrology

Two quantum standards already established in metrology – the Volt based on the Josephson Effect and the Ohm based on the Quantum Hall Effect – crucially relies on the assumption that the relations $K_J = 2e/h$ for the Josephson Constant and $R_K = h/e^2$ for the von-Klitzing Constant hold exactly. Here, e is the elementary charge, and h is the Planck constant.

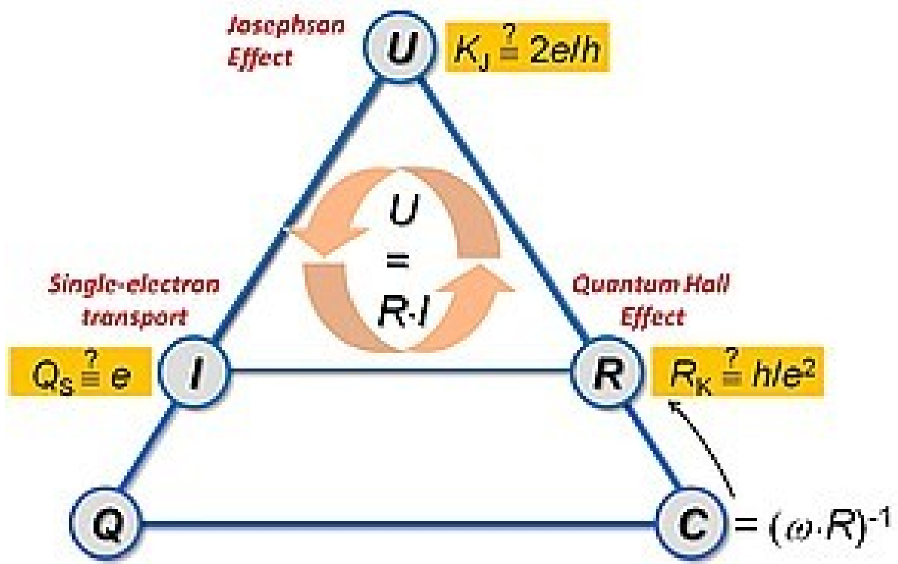

- Quantum Hall Resistance Metrology
- Quantum Josephson Voltage Metrology
- Quantum Current/ Quantum Phase Slip

Quantum Programmable Josephson Voltage Standard

Quantum standards are the measurement systems based entirely on the fundamental properties. These are used for various metrology applications because of their ***highest accuracy and error-free measurement capabilities.***

Established PJVS system at CSIR-NPL India for quantum DC voltage metrology

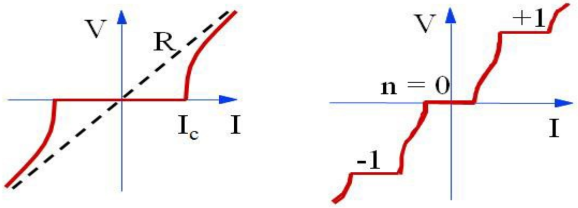

The current-voltage (I-V) curve of a non-hysteretic junction (left without microwave and right with microwave applied).

At CSIR-NPL, one such Quantum standard has been established as the 'Programmable Josephson Voltage Standard' system, which serves as the primary standard of voltage. This system plays an important role in electrical metrology as it is used to disseminate unit 'Volt' throughout the nation to maintain traceability. The quantum accuracy of voltage levels in this system is derived from the 'Josephson Effect', due to which the superconducting junction in the PJVS circuit produces a voltage precisely proportional to the frequency of the applied microwave bias signal. The established quantum standard of voltage always produces an accurate voltage level regardless of environmental conditions or location in contrast to artifacts standards based on electrochemical batteries.

All electrical measurements are traceable to 2 quantum standards:
- **The Quantum Hall Effect (QHE) Resistance Standard And**
- **The Josephson Voltage Standard (JVS).**

Quantum Hall Effect

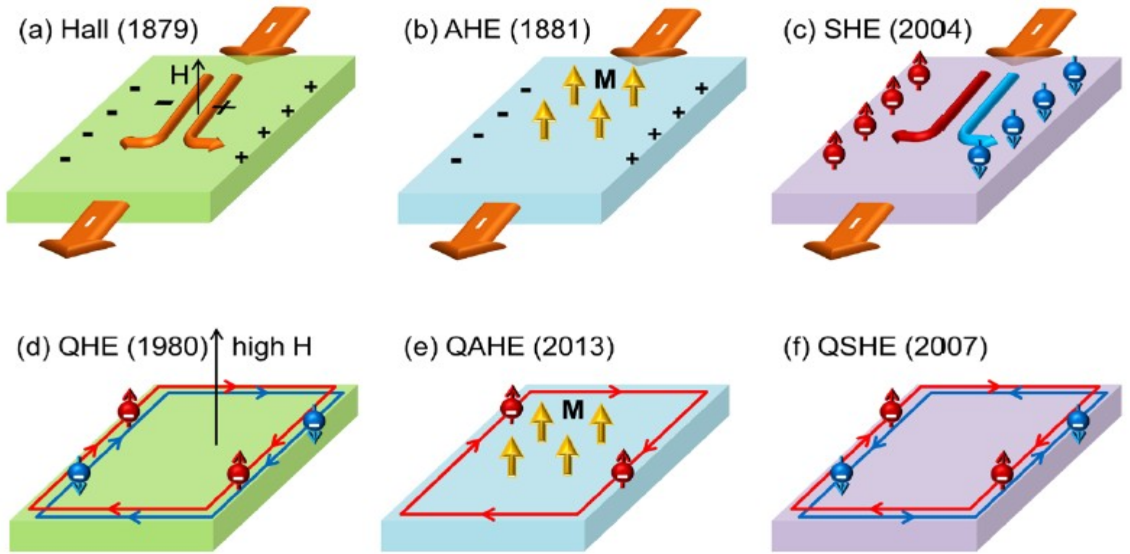

Hall Effect: When electric current flows through a conducting material placed in a perpendicular external magnetic field, the charge carriers that constitute the current are pushed toward the side of the sample by Lorentz force. Therefore, a transverse voltage, named Hall voltage, is developed across the sample.

QHE: In a strong external magnetic field, the continuous density of states of the two-dimensional electron gas (2DEG) split into equally spaced Landau levels. When the Fermi level of the system lies between two neighboring Landau levels, the bulk carriers are localized, but the electrons can propagate along the edge of the sample. The Hall resistance forms well-defined plateaus and the longitudinal resistance ideally becomes zero.

- ❑ QHE was observed in 2DEG system such as graphene, GaAs/AlGaAs and GaN/AlGaN structures, etc. QHE is a consequence of the formation of well-defined Landau levels in presence of high magnetic field, it mostly occurs in those systems in which electron mobility is high.
- ❑ **QAHE:** It has been perceived that in some insulating ferromagnets, the realization of QHE without applying any magnetic field is possible: **Magnetic doped topological insulators**

C.Z. Chang et al. J. Phys.: Condens. Matter 28 (2016) 123002

Quantum Hall Effect (QHE)

- **QHE is a characteristic of a perfectly quantized 2-dimensional electron gas (2DEG) system realized in GaAs/AlGaAs, Graphene, etc. at low temperatures and high magnetic field.**
- **In a strong external magnetic field, the continuous density of states of the 2DEG split into equally spaced Landau levels. When the Fermi level of the system lies between two neighboring Landau levels, the bulk carriers are localized, but the electrons can propagate along the edge of the sample. The Hall resistance forms well-defined plateaus and the longitudinal resistance ideally becomes zero.**

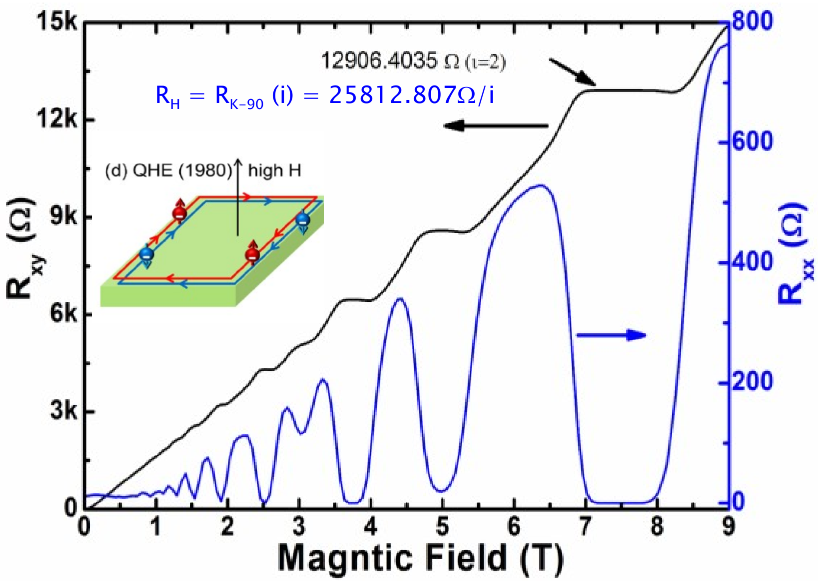

Longitudinal and transverse (Hall) resistance of a GaAs-$Al_xGa_{1-x}As$ (x=0.3) device measured at 1.3 K at CSIR-NPL

- **AQHE: It has been perceived that in some insulating ferromagnets, and magnetic doped TI the realization of QHE at low or without applying any magnetic field is possible.**

Quantum Hall Resistance Metrology

- ✓**The National Ohm** (Ω, the unit of derived parameter 'Resistance') is realized through the Integer Quantum Hall Effect (IQHE) of a perfectly quantized 2-dimensional electron gas (2-DEG) system as GaAs/AlGaAs heterostructures.
- ✓For metrological applications **electron density is of the order of ~ 3-5 x 10^{11}/cm^2** and **electron mobility is higher than ~ 1x10^5cm^2/V.s.**
- ✓The Quantized Hall resistance is given by

$$R_H = R_{K-90} = \frac{h}{ie^2} = 25812.80745\,\Omega\,.$$

- ✓The current devices at NPL are **GaAs/AlGaAs quantum wells**.
- ✓Typical realization is through the measurement of the resistance ratio of a 100 Ω/1000 Ω resistor and the resistance value at the $i = 2$ plateau using a CCC/DCC bridge.
- ✓At CSIR-NPL 1000 Ω resistor is measured with the resistance value at the $i = 2$ plateau using a DCC bridge with an uncertainty of 80 ppb. **(CMC)**
- ✓Quantum Hall Resistance Metrology was established in 2003 and has been peer-reviewed in 2005 and 2010.

Primary Resistance Standard at CSIR-NPL provides resistance traceability to Temperature, DC and LF/HF standard at CSIR-NPL which disseminates to respective industries.

QHR Device: GaAs-Al$_x$Ga$_{1-x}$As (x=0.3) Quantum Well (@ CSIR-NPL)

GaAs (1.5eV) is lightly p-doped
AlGaAs (2.2eV) is n-doped
Mobility (μ) ~ 10-20 T^{-1}
Carrier concentration (n) ~ 3-6 x 10^{15} r
Magnetic Field (B)~ 7-9 Tesla

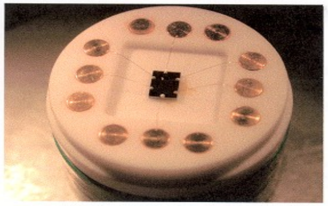

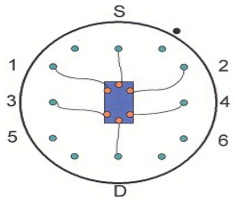

GaAs-Al$_x$Ga$_{1-x}$As (x=0.3) device mounted on a TO-8 holder with contacts and contact geometry

Quantum Hall Resistance Metrology

When QHR device (GaAs-AlGaAs) cooled to a very low temperatures ~ 1.5 K and at a high magnetic field (6-12 T), perpendicular to the layer of 2DEG, yields Quantized Hall Resistance (R_H). A series of steps (plateaus) appear in the Hall (transverse) Resistance as function of magnetic field. Concomitantly the longitudinal resistance accurately falls to zero at the centre of each plateau and oscillates to a n[illegible]lue between the plateaus. The plateaus occur at incredibly precise value of resistan[illegible]y

$$R_H = \frac{1}{i}\frac{h}{e^2}$$

where 'h' is the Planck constant (6.626 070 15 x 10^{-34} Js) , 'e' is the electronic charge (1.602 176 634 x 10^{-19} C), 'i' is an integer and 'R_{K-90}' is the Klitzing constant (25812.807 459 3045).

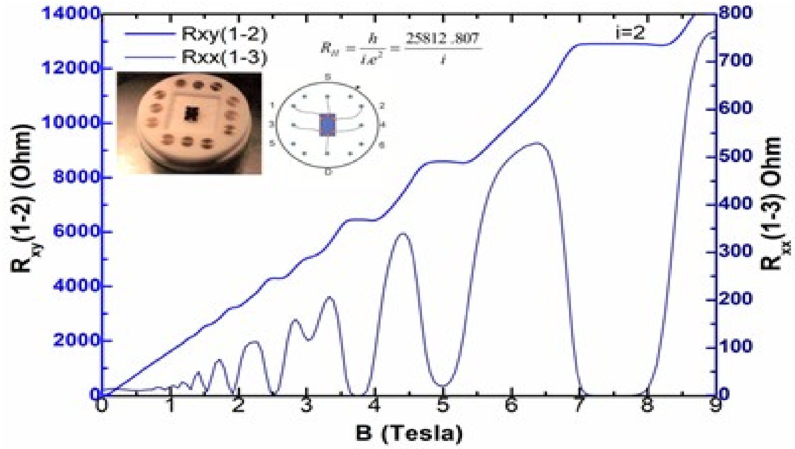

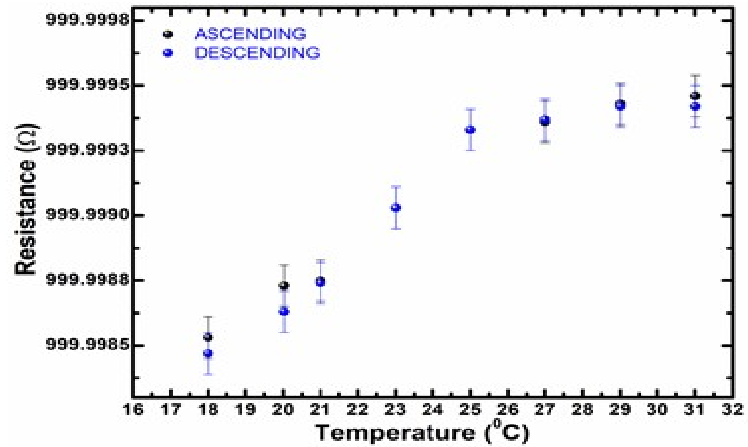

Magnetic field dependence of the Hall and longitudinal resistance of the perfectly quantized 2D electron gas & comparison of 1000 Ω Standard with R_{K-90}(i=2) = 12906.40373 Ω using the DCC bridge

Quantum Materials: Topological Insulators

Primary Resistance Standard i.e. Quantum standard for electrical resistance is based on the **Quantum Hall effect (QHE)** of quantized two-dimensional electron gas (2DEG) realized in semiconductor heterostructures (GaAs/AlGaAs quantum wells).

Few critical issues:

- Creation of 2DEG required sophisticated and costly equipment
- Stringent measurement conditions such as low temperature and high magnetic fields.

Alternatives:

Magnetically doped topological insulators (MTI) appear to be the germane class for realization of cost-effective quantum standard under relaxed and less stringent measurement conditions.

Topological Insulators: Background

Electronic states of matter

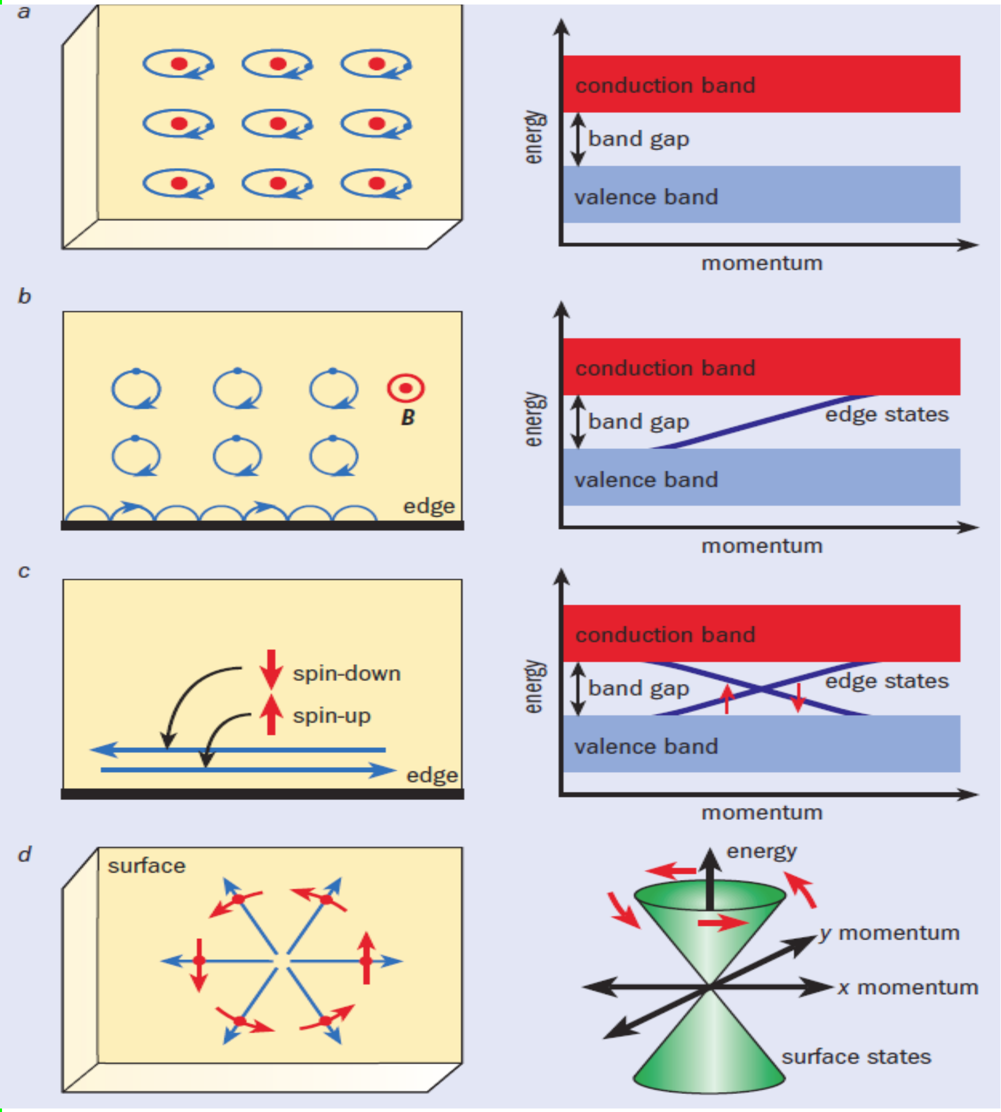

M. Z. Hasan et al Rev. Mod. Phys. 82 (2010) 3045.

(a) Insulating state is characterized by an energy gap separating the valence and conduction band

(b) In Quantum Hall effect, circular motion of electrons in a magnetic field is interrupted by sample boundary. At the edge, electrons execute skipping orbitals, leading to conduction in one direction along the edge.

(c) Edge of quantum spin Hall effect or 2D TI contains left- and right-moving modes with opposite spin and related by time-reversal symmetry. Similar to half of a quantum wires with spin-up and spin-down electrons propagating in both directions.

(d) The surface of a 3D TI supports electronic motion in any direction along the surface, but the direction of the electron's motion uniquely determines its spin direction and vice versa. The 2D energy-momentum relation has a "Dirac cone" structures.

Topological Insulators: Background

The Topological insulators (TIs) are the new state of quantum materials in which their robust surface states are protected by time-reversal symmetry and induced by strong spin-orbit coupling.

The bulk of the material behaves as an insulator, while its surface or edges host conducting states due to non-trivial electronic band topology.

TI surface states are extremely robust against scattering by non-magnetic impurities and surface distortion.

Edge of quantum spin Hall effect or 2D TI contains left- and right-moving modes with opposite spin and related by time-reversal symmetry.

The surface of a 3D TI supports electronic motion in any direction along the surface, but the direction of the electron's motion uniquely determines its spin direction and vice versa. The 2D energy-momentum relation has a "Dirac cone" structure.

M. Z. Hasan et al Rev. Mod. Phys. 82 (2010) 3045.

Topological Insulators: Background

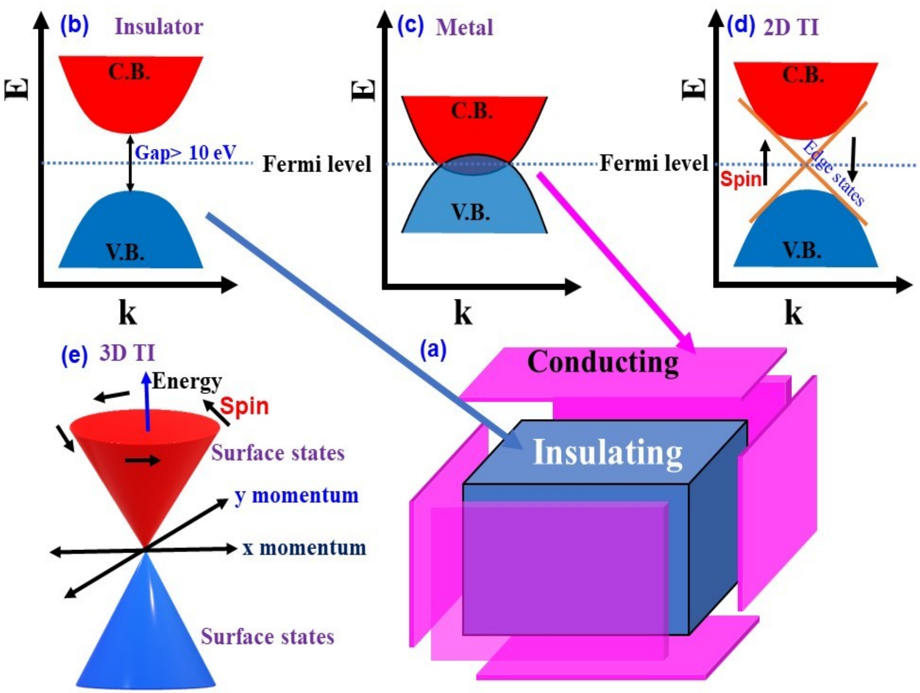

Kane et al. Phys. Rev. Lett. 95 (2005) 226801

M. Z. Hasan et al Rev. Mod. Phys. 82 (2010) 3045.

Zhang et al. Science 314 (2006) 1757

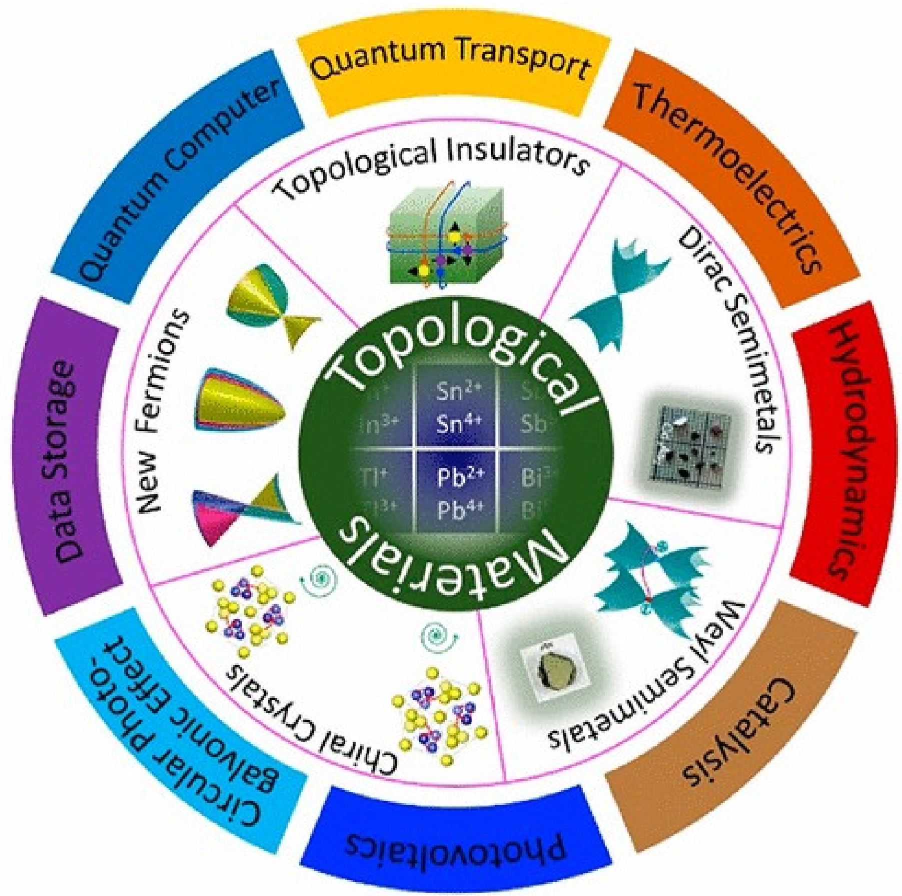

Application of topological insulators

Characterization Techniques of TIs

- Angle-Resolved Photoemission Spectroscopy (ARPES)
- **Scanning Tunnelling Microscopy (STM)**
- Transport measurements (PPMS, Hall etc)
- Optical method (Raman, Ultrafast spectroscopy etc)

➢ ARPES is a powerful technique that directly probes the electronic band structure of materials. It involves shining photons (typically ultraviolet or X-rays) on a sample and measuring the kinetic energy and momentum of the emitted electrons.

➢ For topological insulators, ARPES can reveal the presence of Dirac cones, which are characteristic of the topological surface states.

➢ The measured band structure provides information about the dispersion and Dirac point location of these surface states.

Single crystal of Bi_2Se_3

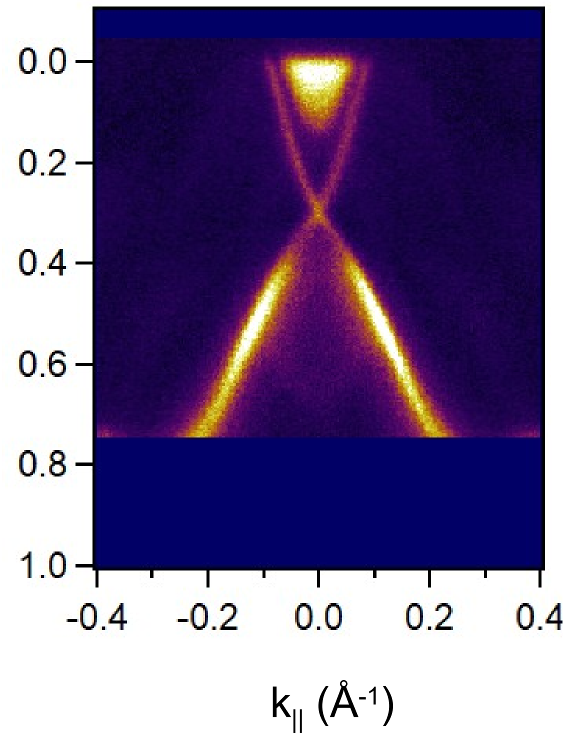

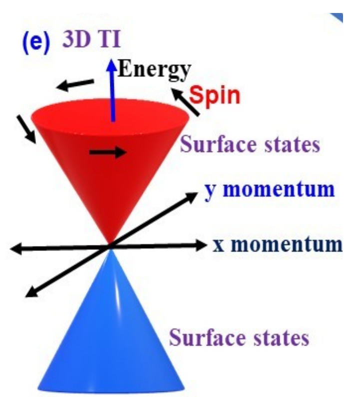

Quantum based characterization technique

❑ Scanning tunneling microscopy (STM)

Based on quantum mechanical tunneling effect

Objects as classical particle : Defined mass and energy

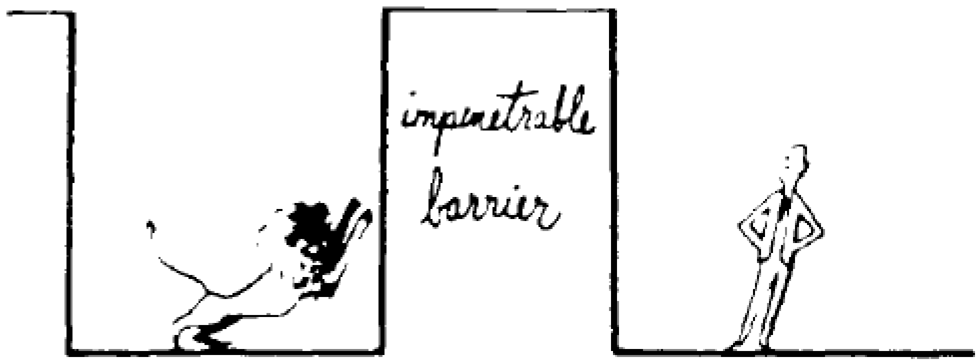

If it were to be a quantum particle ?

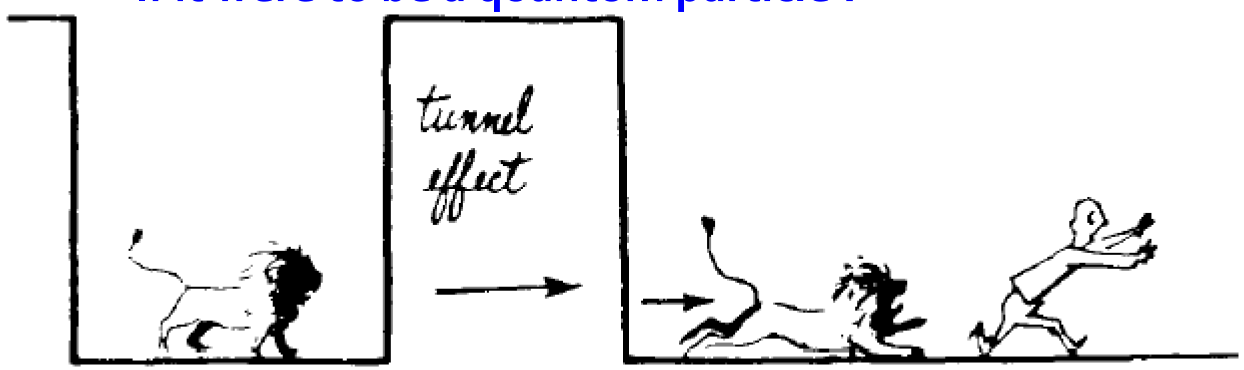

This illustration was used by Van Vleck in his last publication, the Julian E. Mack Lecture at his Alma Mater, the University of Wisconsin, in 1979. B. Bleaney. Contemp. Phys. 25 (1984) 320.

Scanning Tunneling Microscopy (STM)

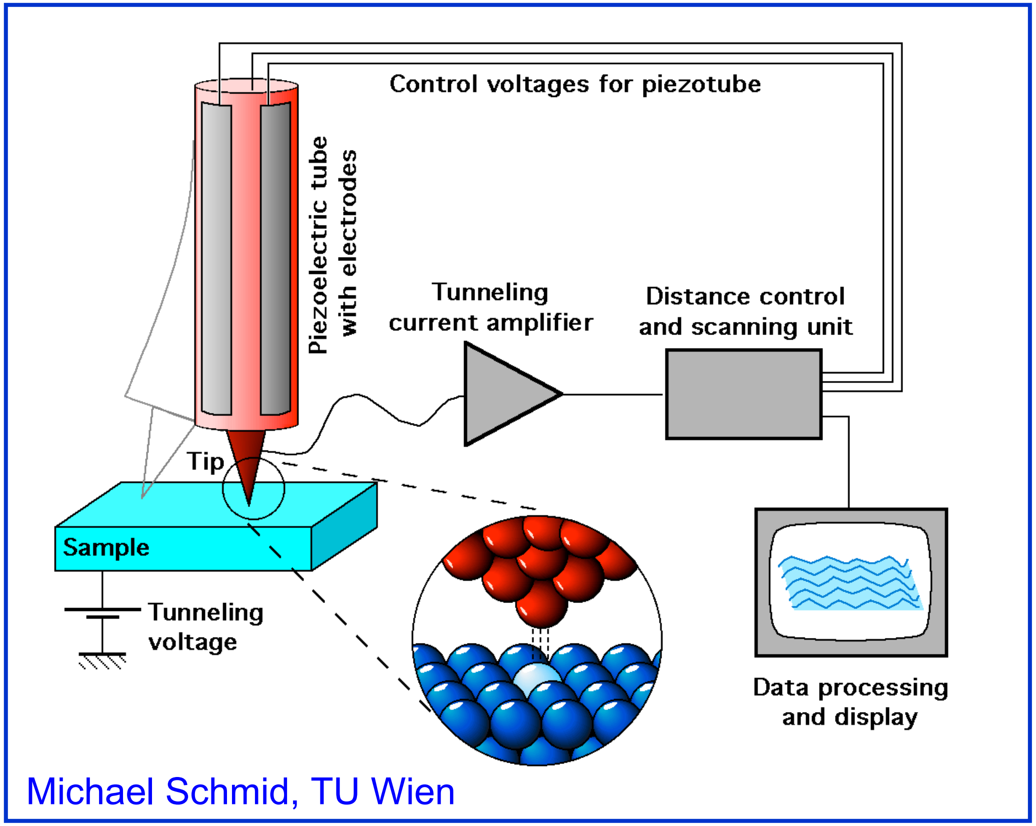

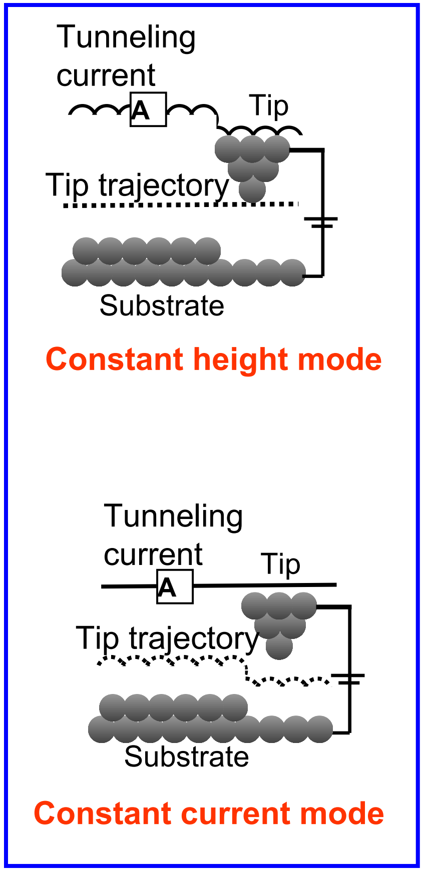

$$I_t \propto V \exp(-A\varphi^{1/2}d)$$

Operational Mode

I_t : the tunnel current, a sensitive function of the gap width d ; V: the bias voltage; φ: the average barrier height (work function) ; A: constant = 1.025 $eV^{-1/2}$ Å^{-1}.

Resolution limit: 0.1 nm (Lateral), 0.01 nm (Vertical)

Scanning Tunneling Microscopy (STM)

Working principle of STM

- The vacuum serves as a potential barrier in STM, when the sharp metallic tip is brought very close to a conducting sample.

- If a small positive sample bias (with respect to tip) is applied ($V < \varphi_s$), the Fermi energy of the tip will be shifted upward and electrons will tunnel from the occupied states of the tip to the unoccupied states of the sample. (Empty state imaging)

- If a small positive voltage is applied to the tip with respect to sample, electrons will tunnel from the occupied states of the sample to the unoccupied states of the tip. (Filled state imaging)

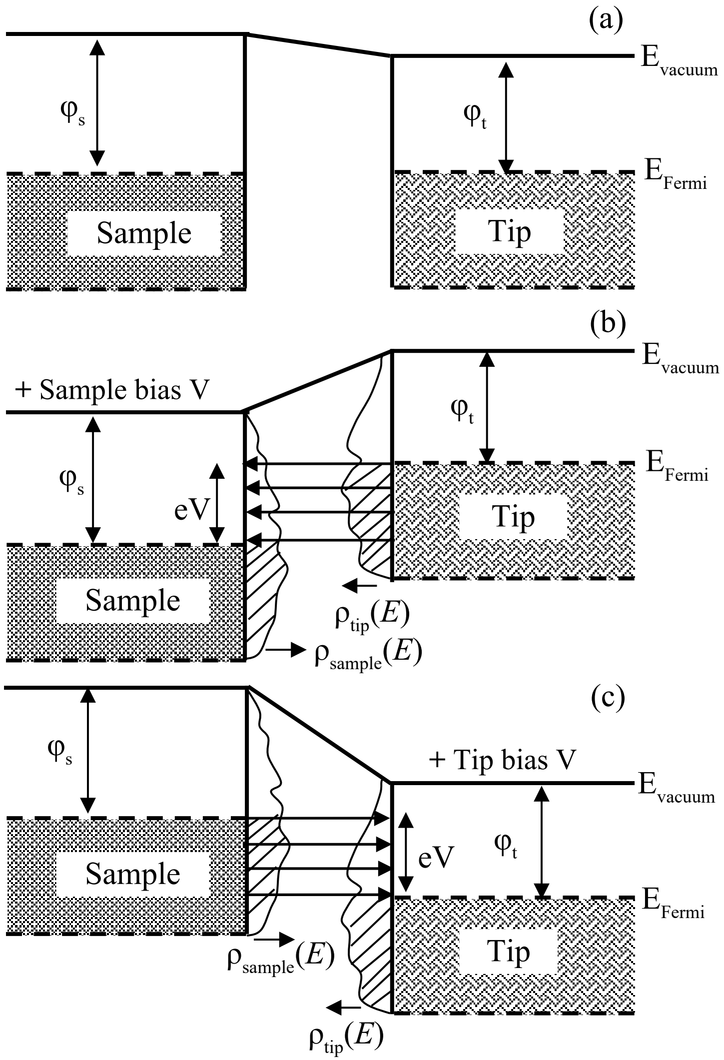

(a) Energy band diagram of STM tunnel junction at equilibrium; (b) when positive small sample bias voltage is applied and (c) when positive tip voltage is applied.

Scanning Tunneling Microscopy (STM)

❑ Example of Filled and Empty STM images

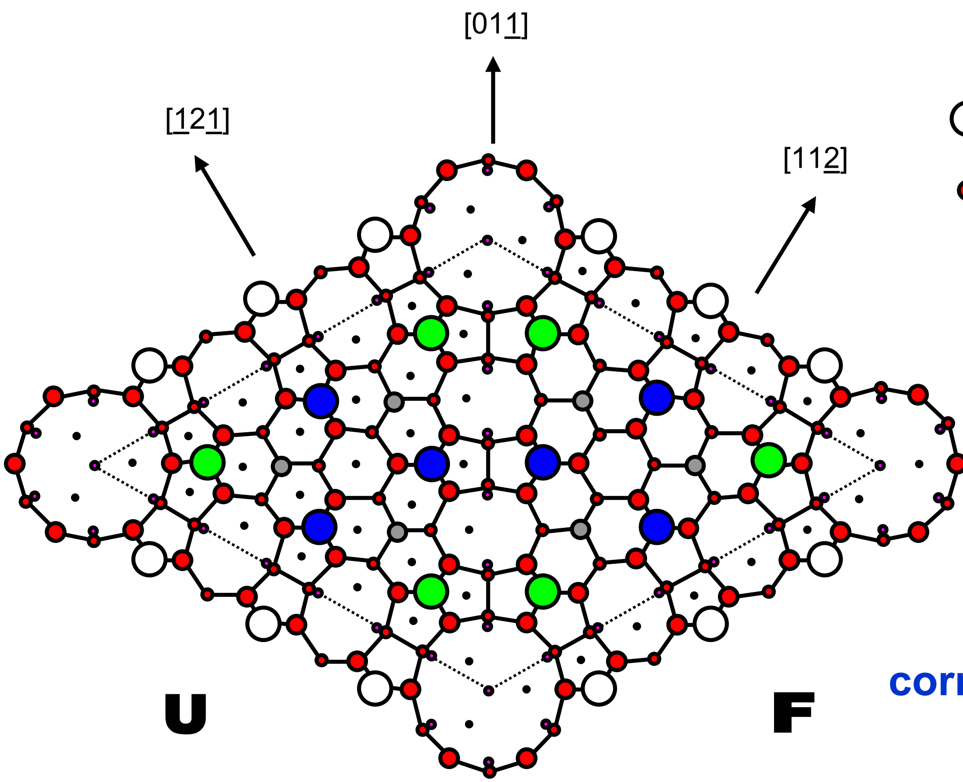

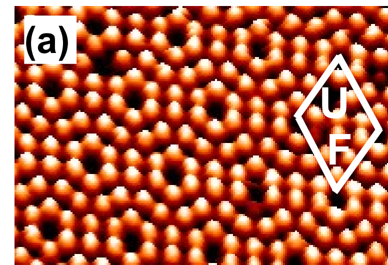

Empty state

corner adatom

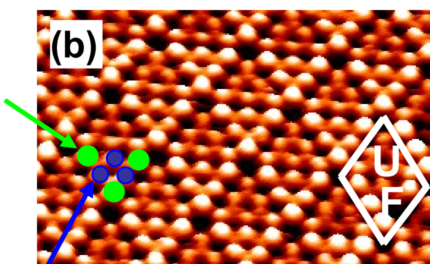

Filled state

center adatom

Dimer-adatom-stacking-fault (DAS) model for Si(111)-7×7 reconstruction & STM image

Why Sb and Bi on Inert substrates?

- Sb, Bi and their alloys are shown the topological insulator behaviour.

X. S. Wang, Nano Lett. 2015, 15, 80–87

- Nanostructures grown on metal or semiconductor surface can form interfacial alloys.

Surf. Sci. 415, (1998) 106, Phys. Rev. B 63, (2001) 193301

➢ To reveal high purity & intrinsic properties of nanostructures, inert substrates are suitable due to minimal interface effect.

Appl. Phys. Lett. 88 (2006) 233105, Phys. Rev. Lett. 96 (2006) 86104

❖ Highly oriented pyrolytic Graphite (HOPG)

- Inert substrate
  - Suitable for nearly free standing nanostructures
- Atomically flat surface
- Layered structures
- Easy to prepare clean surface

❖ Molybdenum disulphide (MoS_2)

have atomically flat surface ~ 2- 4 µm

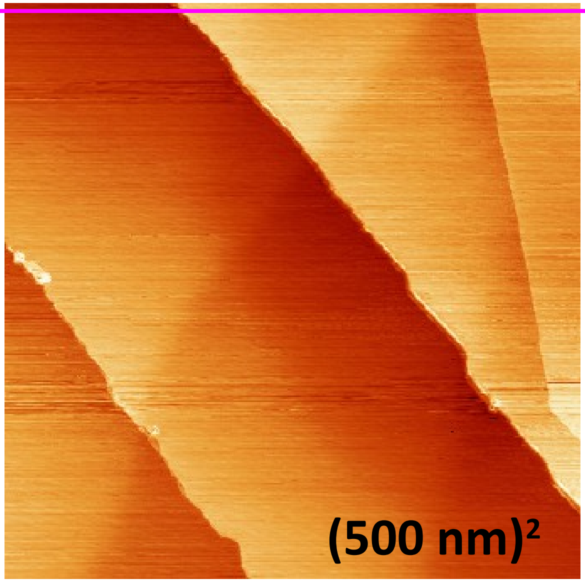

STM image of clean HOPG

Ultra-high vacuum STM system

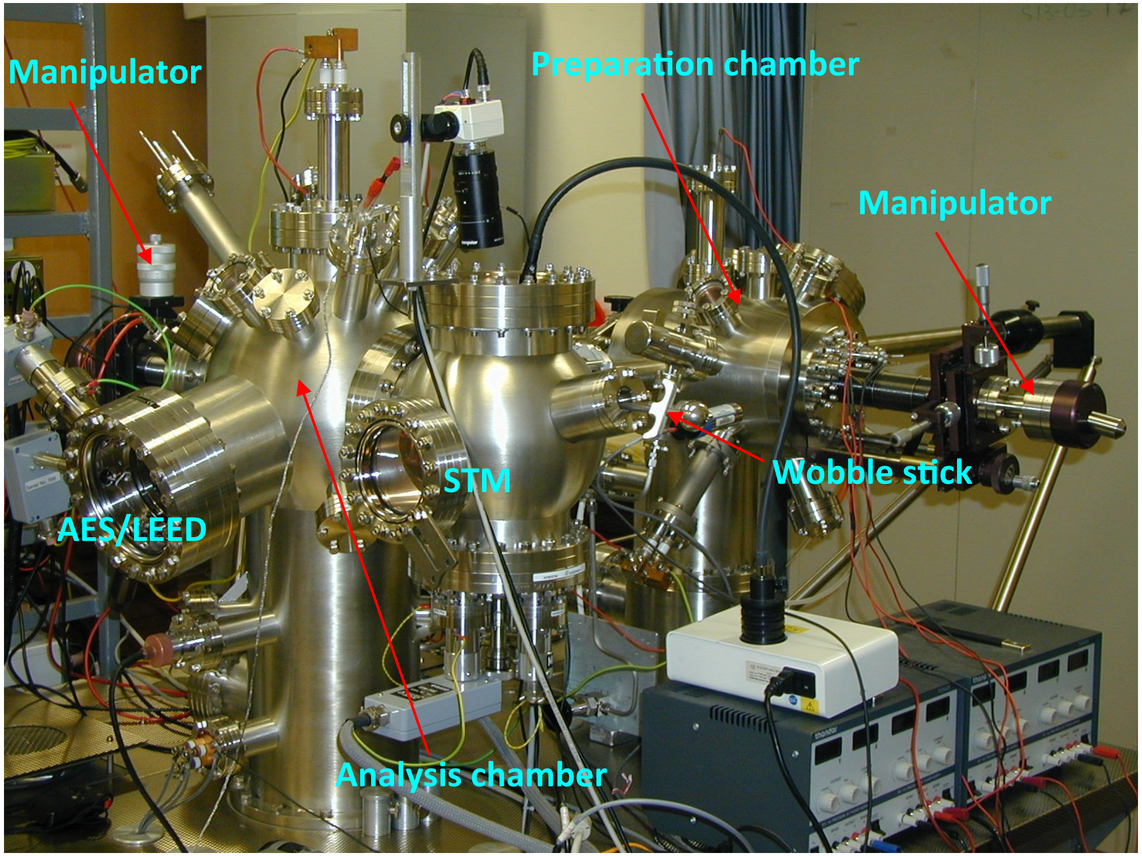

Multi-chamber Omicron UHV system equipped with STM, LEED and AES

- Base Pressure ~ 2×10^{-10} mbar
- Sb (mostly Sb_4) and Bi evaporator sources
- Flux calibrated with STM and Auger electron spectroscopy (AES)
- Sample heater
- STM images at room temperature (RT)

Cleaning process of HOPG

- Cleave HOPG/MoS_2 in air
- Quickly transferred in UHV
- Degassed at 800/600 K for ~ 8 hrs

Different dimensionality Sb islands on Graphite

Three types of Sb structures on HOPG:

3D, 2D and 1D structure

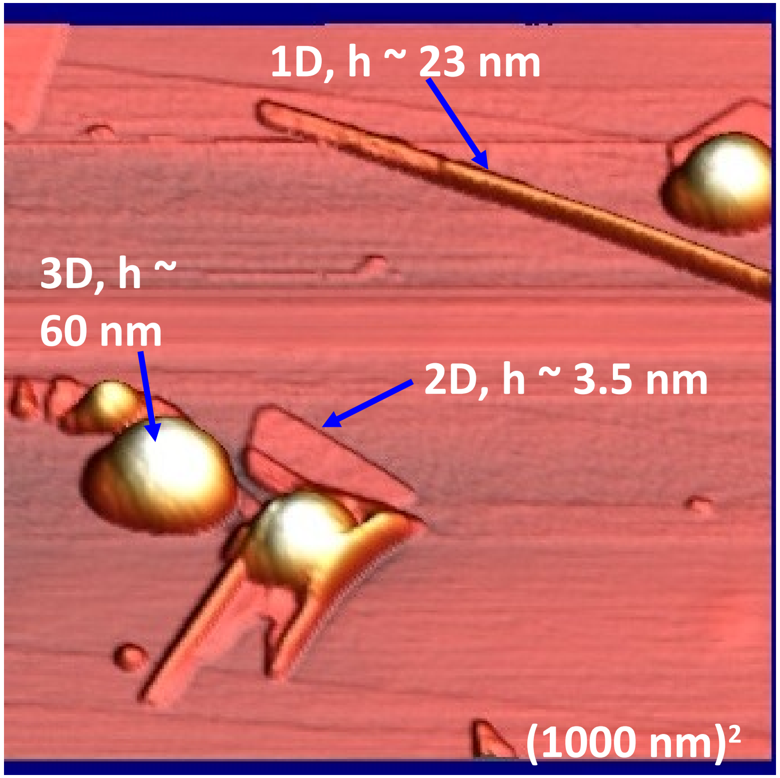

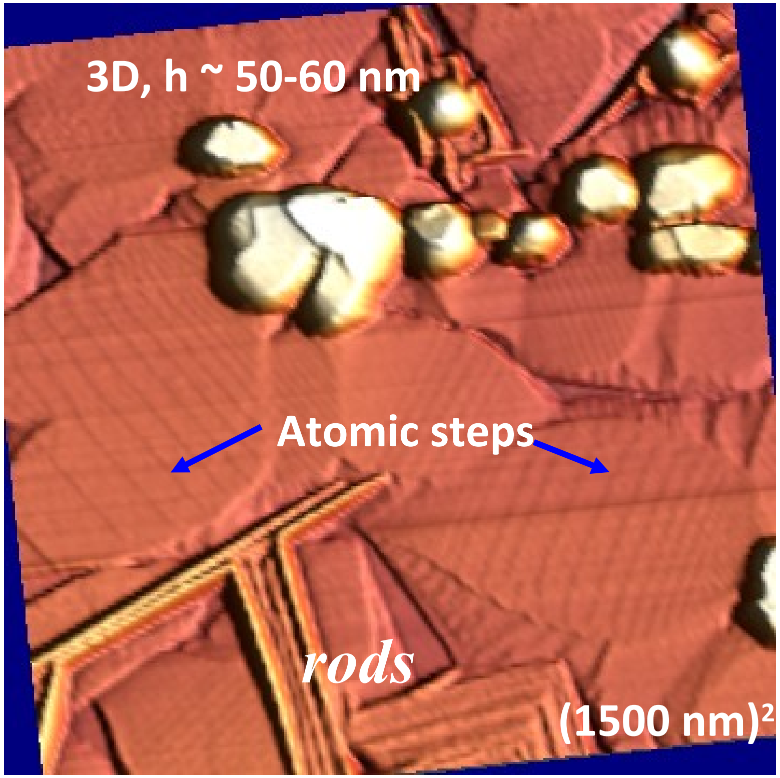

1.2-nm Sb deposition at flux ~ 4 Å/min at RT

3D, 2D & 1D islands formed in early stage

10-nm Sb deposition at RT

Facets on 3D islands

2D and 1D structures grow dominantly in later stage

Crystal structures of Sb and Bi

Rhombohedral (RHL) Structure

α-Sb

a_{rh} = 4.51 Å

c = 11.27 Å

α = 57.11°

α-Bi

a_{rh} = 4.75 Å

c = 11.86 Å

α = 57.23°

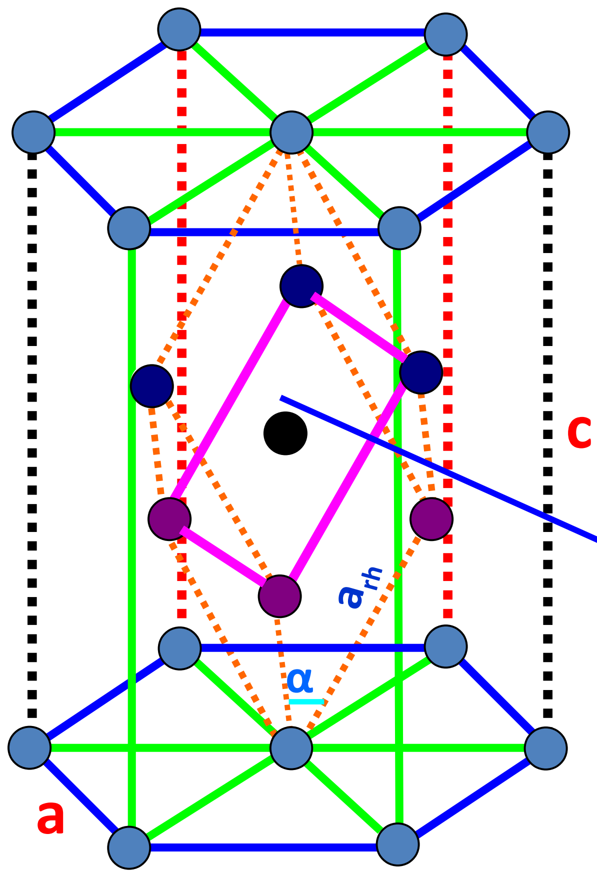

α-Sb(111)

a= 4.31 Å

α-Bi(111)

a= 4.54 Å

1st layer

2nd layer

3rd layer

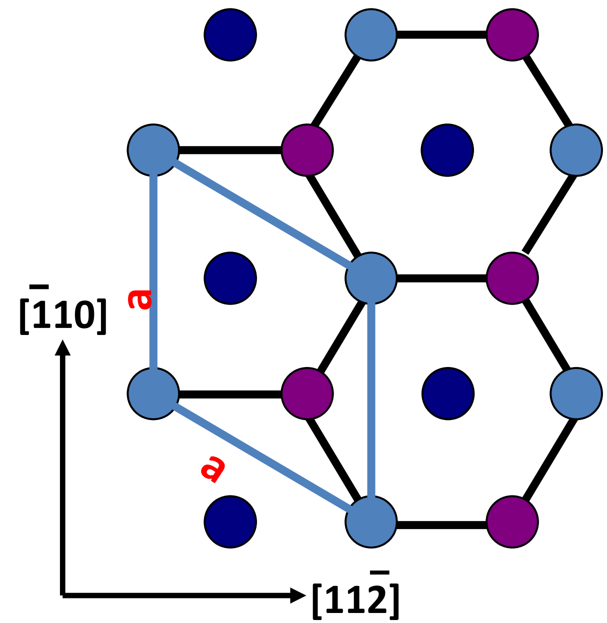

α-Bi(110)

4.54 Å×4.75 Å

α-Sb(110)

4.31 Å×4.51 Å

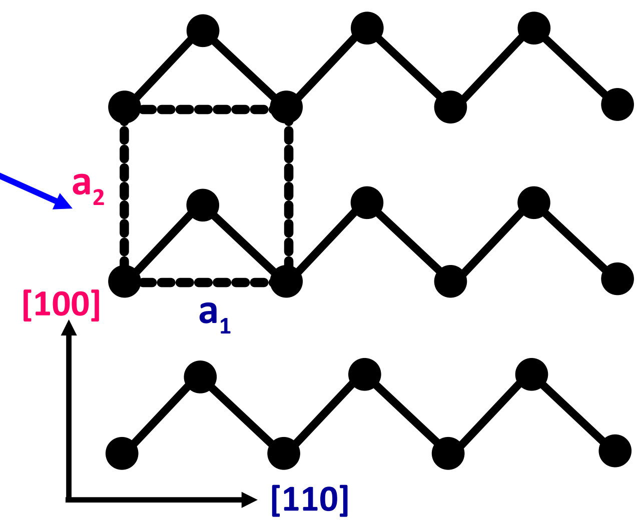

J. Donohue, *The Structures of the Elements,* Wiley & Sons, New York, 1974.

3D Sb islands on HOPG

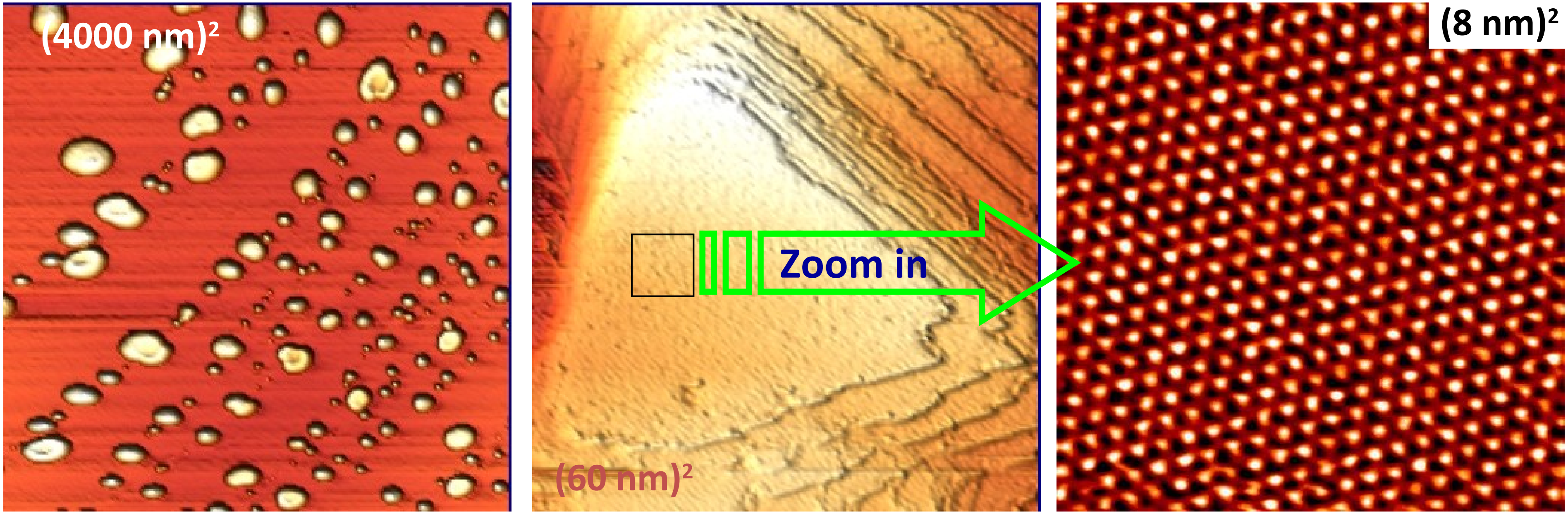

1.8-nm Sb at low flux ~ 1.8 Å/min and at RT

High resolution image on 3D island

- Mostly found along HOPG steps
- Easy coarsening
- Round surface even at large volume
- (111) Facets on top of large islands, hexagonal period 4.28 Å

Hexagonal structure

Lateral period 4.28 Å

α-Sb(111) **a= 4.31 Å**

S.S. Kushvaha *et al*. Nanotechnology 18 (2007) 145501

2D Crystalline Sb structures

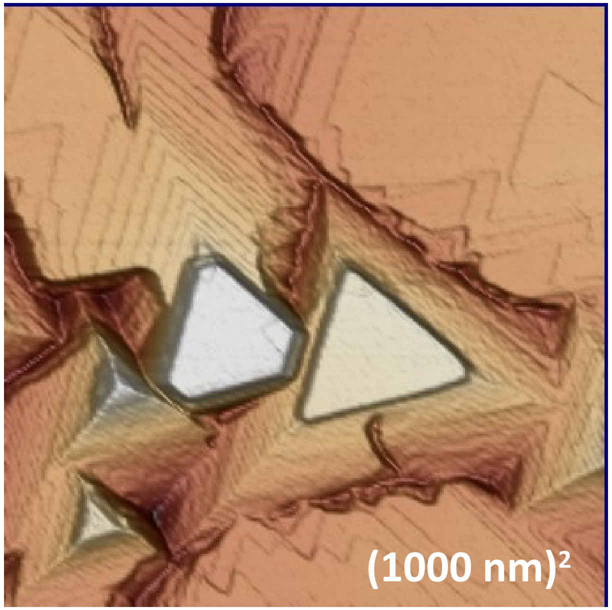

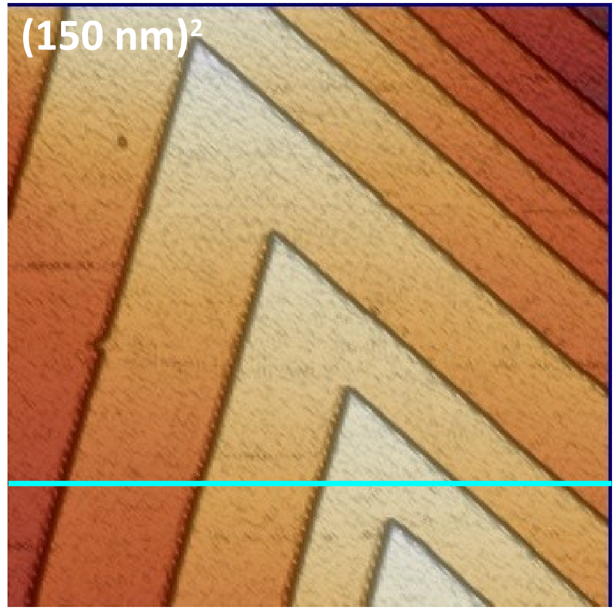

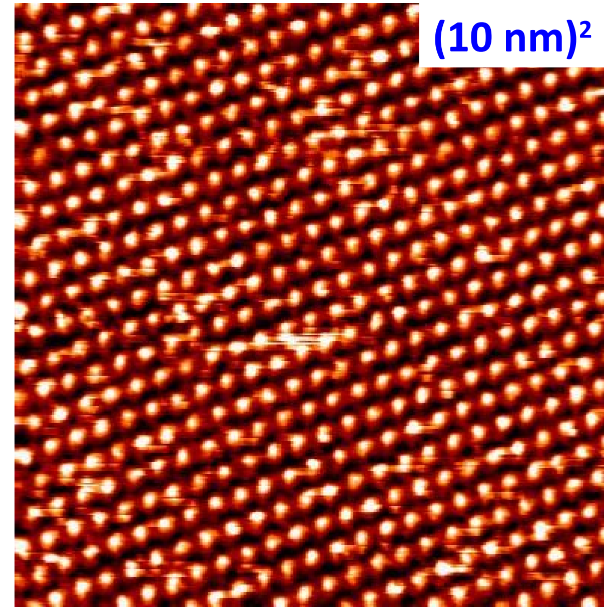

40-nm Sb deposited at flux ~ 20 Å/min at RT

HOPG surface fully covered by 2D multilayer structure

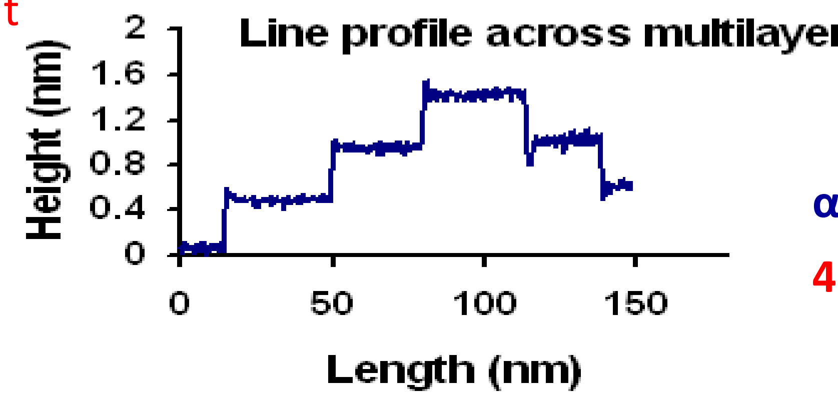

Step height 3.9 Å

Hexagonal ordered structure

Lateral period: 4.17 Å

α-Sb(111): Interatomic spacing 4.31Å, step height 3.75 Å

S.S. Kushvaha *et al*. J. Phys.: Condens. Matter 18 (2006) 3425

Sb Nanorods on HOPG

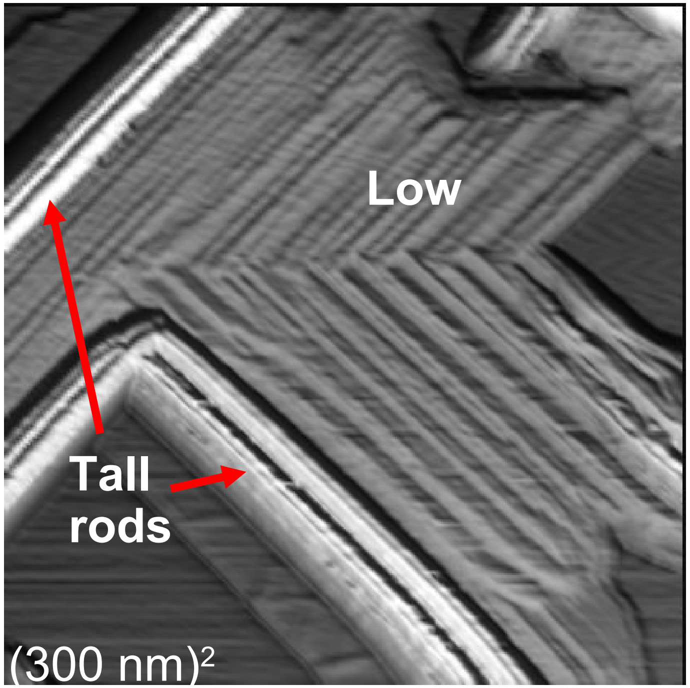

Tall (≥ 20 nm) & Low (≤ 15 nm) NWs, some in "L" shape

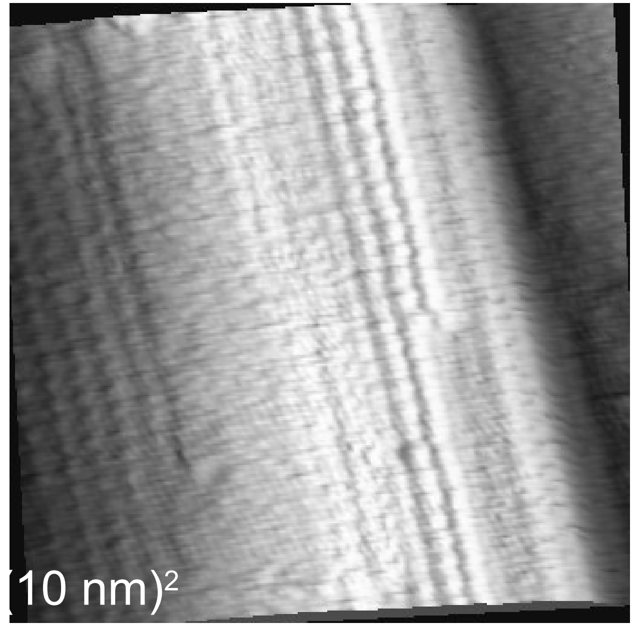

Row structures on tall NWs

Row spacing: 4.5 ± 0.2 Å

Period along row: 3.70 ± 0.15 Å

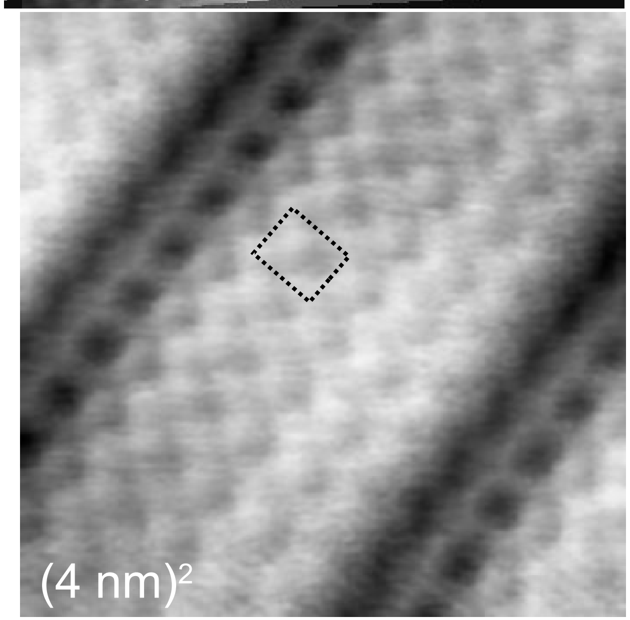

Lower NWs away from corner

Rectangular cell: (4.40±0.15 Å) × (3.93± 0.15 Å)

X.-S. Wang, S.S. Kushvaha *et al*. Appl. Phys. Lett. 88 (2006) 233105

Bi nanostructures on Graphite

Three types of Bi structures on HOPG:

2D, 1D and 1D-multilevel structure

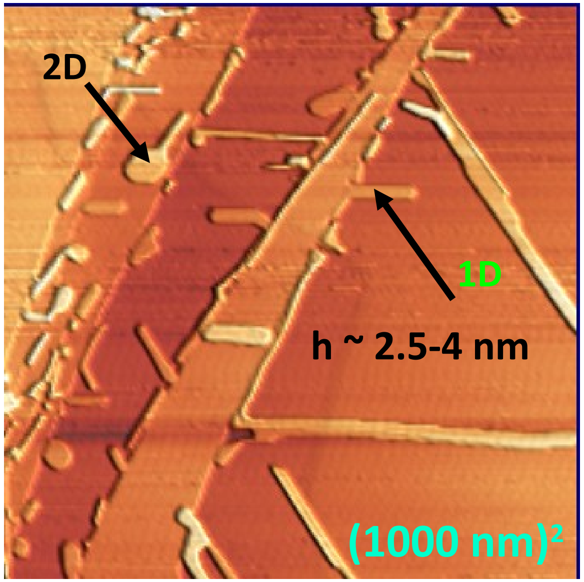

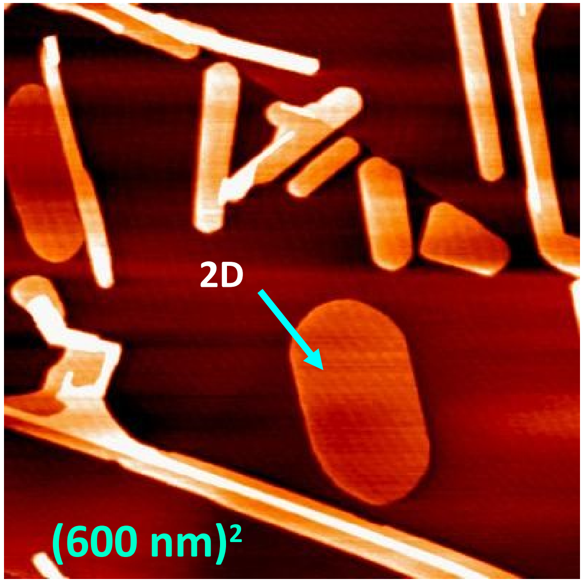

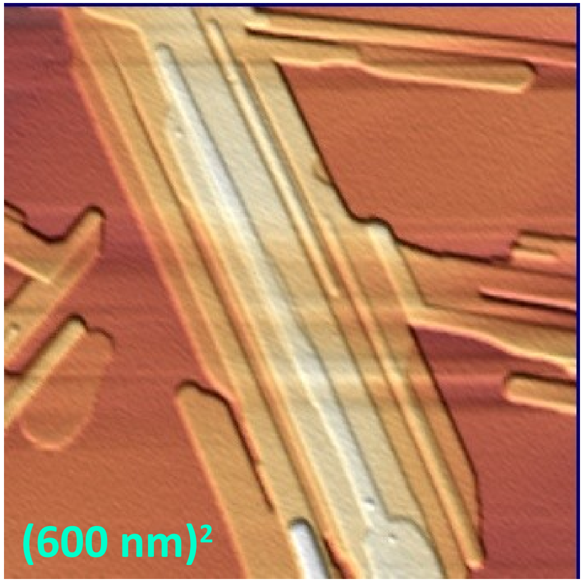

0.4-nm Bi at RT

2D & 1D structures formed in early stage

1-nm Bi deposition with flux of 0.8 Å/min at RT

2D & stripe structures

1.5-nm Bi deposition at RT

Multilevel structures

Height of multilevel ~ 33 Å

Even (10) number of d_{110} (3.28 Å)

No 3D islands were observed as compared to Sb

Bi evaporates as Bi_1 and Bi_2, Sb in form of Sb_4

Selected values of Thermodynamic properties of Metals and Alloy, Wiley, New York, 1963.

Crystalline 2D Bi structure

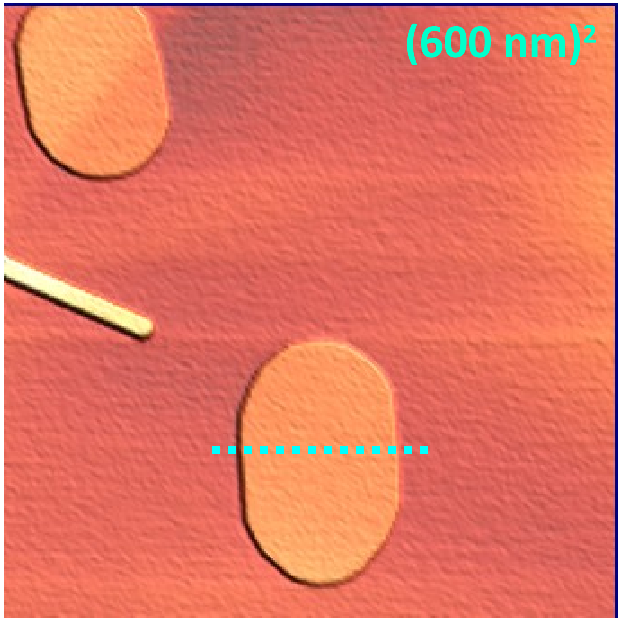

0.8-nm Bi deposition with flux of 0.8 Å/min at RT

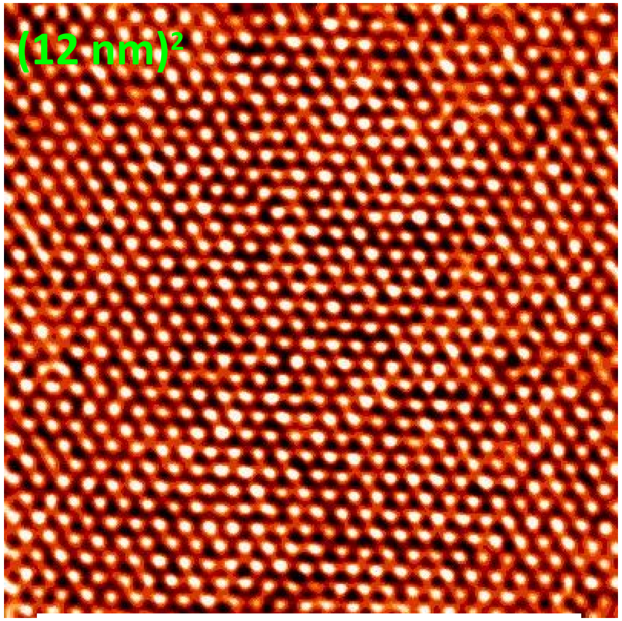

Lateral period: 4.31±0.06 Å

5% less than α-Bi(111)

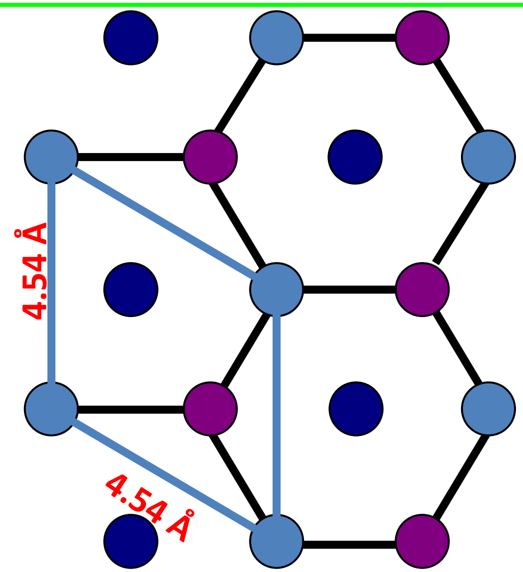

α-Bi(111) : a=4.54 Å

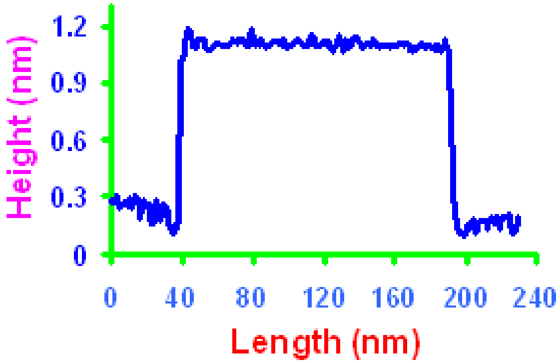

2D structure step height ~ 8±0.8 Å, equal to [2×d_{111}(3.95)] Å= 7.9 Å

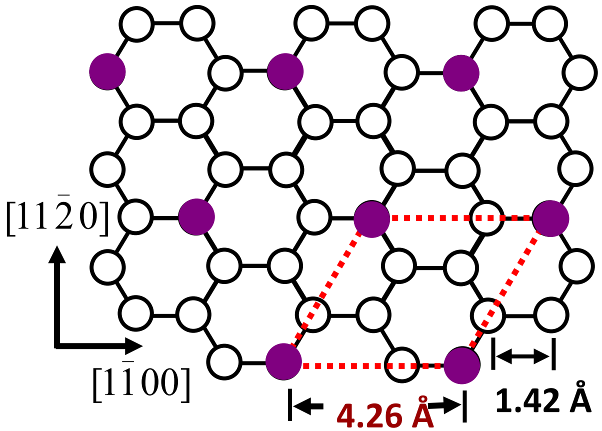

Orientation relationship of α-Bi(111) and graphite (0001)-(√3×√3)R30°

Crystalline 1D and multilevel structure

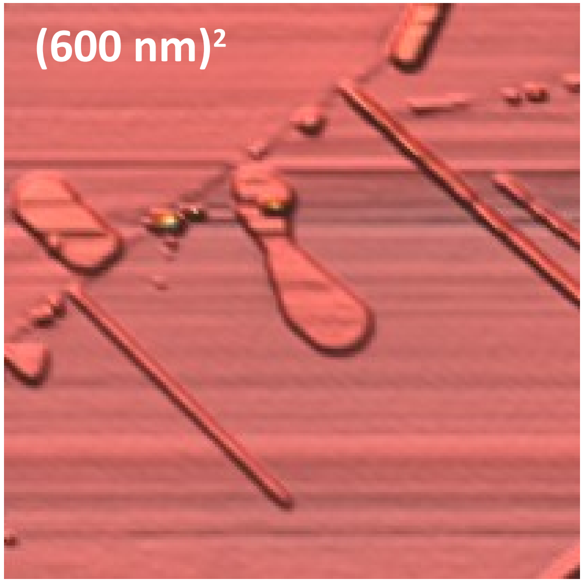

0.3-nm Bi deposition

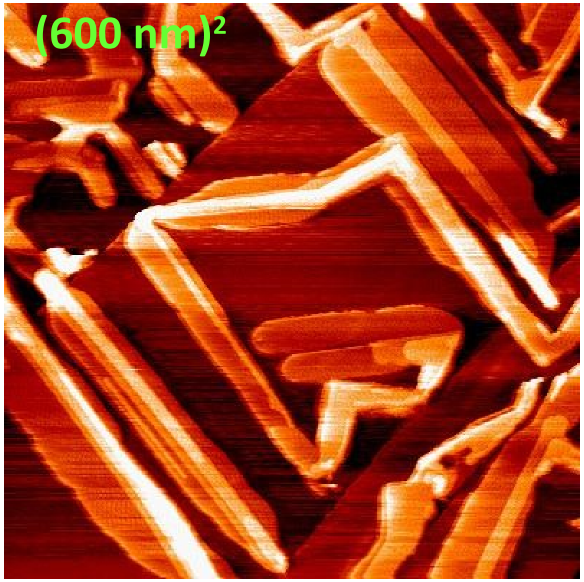

1.2-nm Bi deposition at RT

Multilevel structures

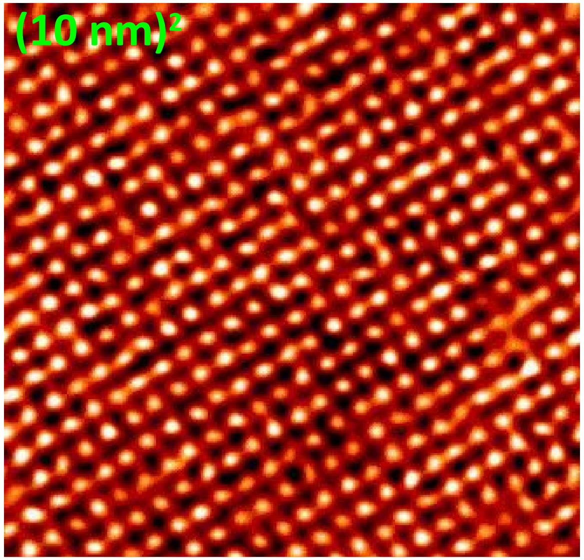

Rectangular Structure

(4.34±0.06 Å) × (4.64±0.08 Å)

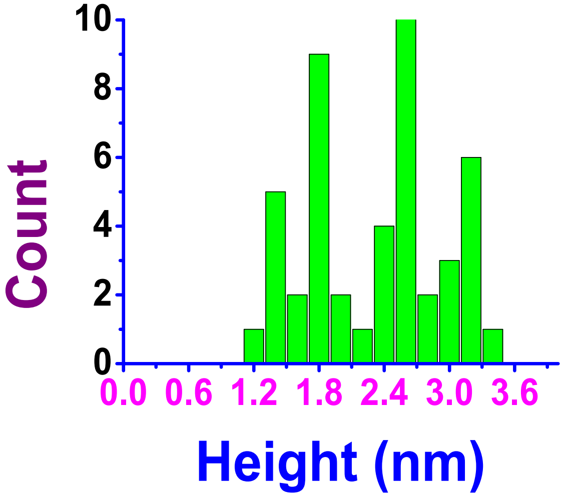

Height of layers are either **13.6 Å or ~ 6.6 Å**

Very close to even number of d_{110} (3.28 Å)

5% less along longitudinal axis whereas 2% less in transverse axis

α-Bi (110) [4.54 Å × 4.75 Å]

Bi on MoS_2 at RT

Elongated 1D nanostructures

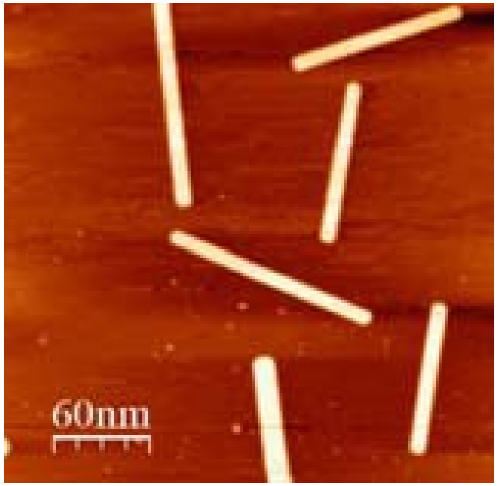

After ~ 0.2 nm Bi deposition at flux 0.6 Å/min

After ~ 0.4 nm Bi deposition at flux 0.6 Å/min

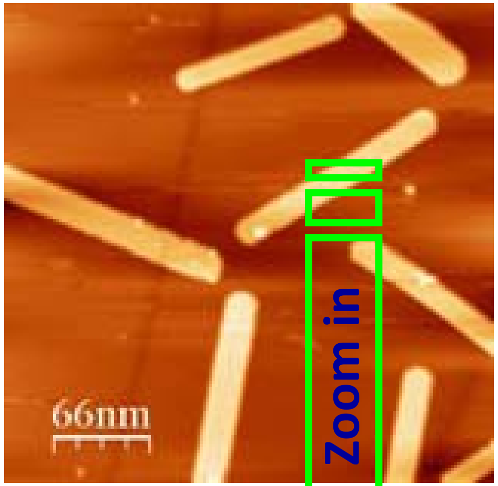

- ***Uniform*** height of 6.6 Å **[2 layer of d_{110} (3.28 Å)]**

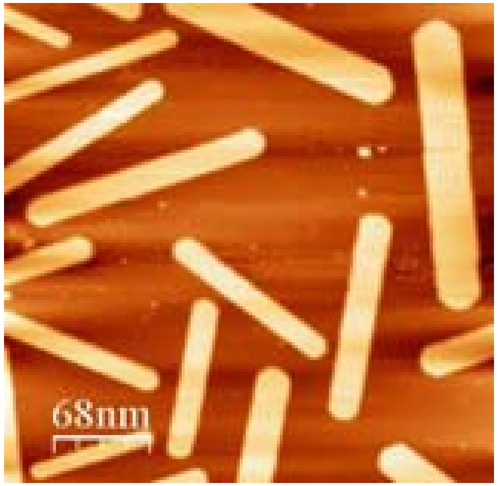

- Angles between the nanoribbons are 0º, 60º or 120º, corresponding to the ***three-fold symmetry*** of the substrate.

After ~ 0.8 nm Bi deposition at flux 0.6 Å/min

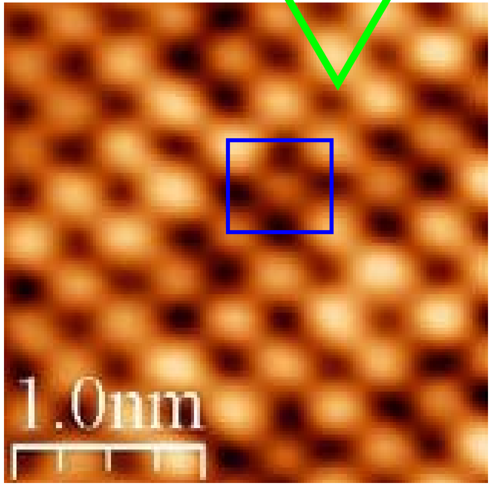

α-Bi (110)

Bi on HOPG: LT STM/STS

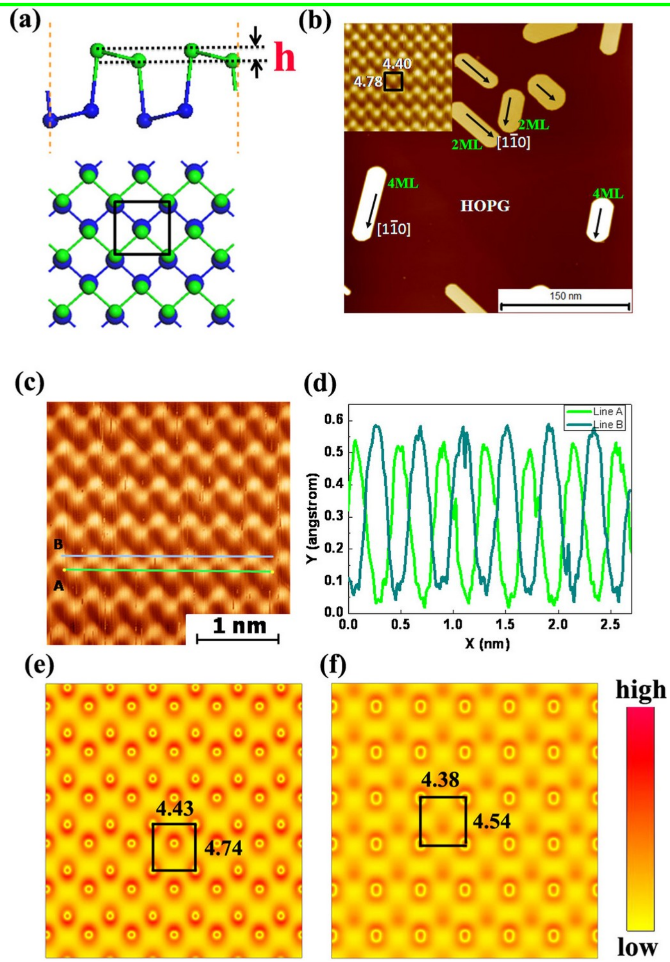

Crystal structure of 2D Bi(110) thin films. (a) Schematic side- and top-views of 2-ML Bi(110) film with up and down layer represented by green and blue balls, respectively. Buckling is defined in terms of the height difference between two atoms of the same monolayer. (b) STM image of Bi(110) film on HOPG (V_s = 2 V, I = 0.01 nA).

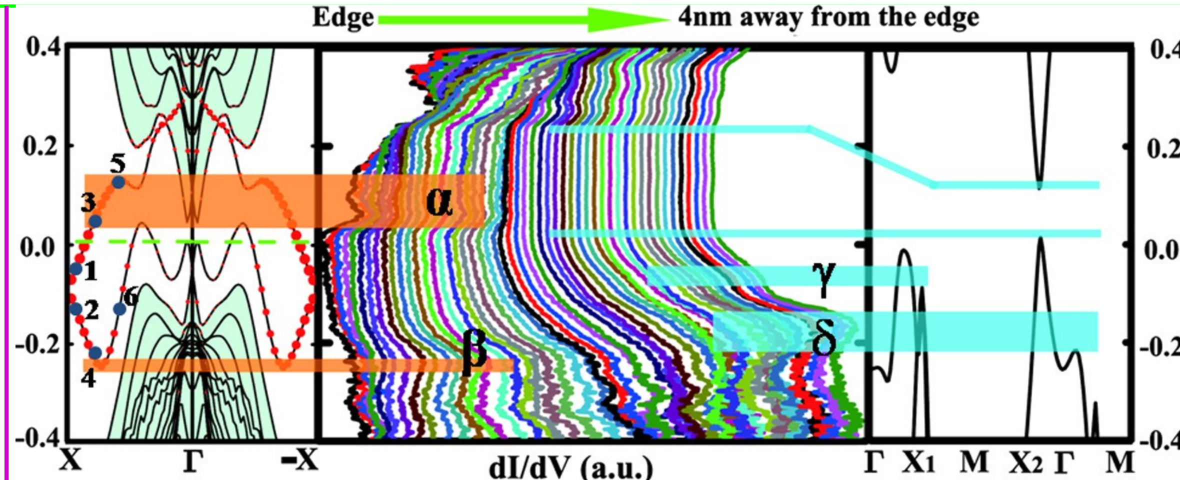

The edge states of 2-ML Bi(110) thin films. Left panel: Calculated band structure of the ribbon with a width of 6 nm. The helical states localized at the edges of the ribbon are visualized by red circles. Bulk states are shaded by green color. E_F is set at E = 0. Middle panel: **STS measured at 4.2 K** from edge to the position 4 nm away from the edge of 2-ML Bi(110). The yellow and blue lines and bar area are guides to the eye, which correspond to characteristic feature in calculated band structure shown in the left and right panel. Right panel: Calculated band structure of infinite large 2-ML Bi (110) film.

First-principles calculations and scanning tunneling microscopy/spectroscopy (STM/STS) experimental studies, we report nontrivial 2D TI phases in 2-monolayer (2-ML) and 4-ML Bi(110) films with large and tunable bandgaps determined by atomic buckling of Bi(110) films. The gapless edge states are experimentally detected within the insulating bulk gap at 77 K. The band topology of ultrathin Bi(110) films is sensitive to atomic buckling. Such buckling is sensitive to charge doping and could be controlled by choosing different substrates on which Bi(110) films are grown.

X. S. Wang, Nano Lett. 2015, 15, 80–87

STM : Atomic manipulation

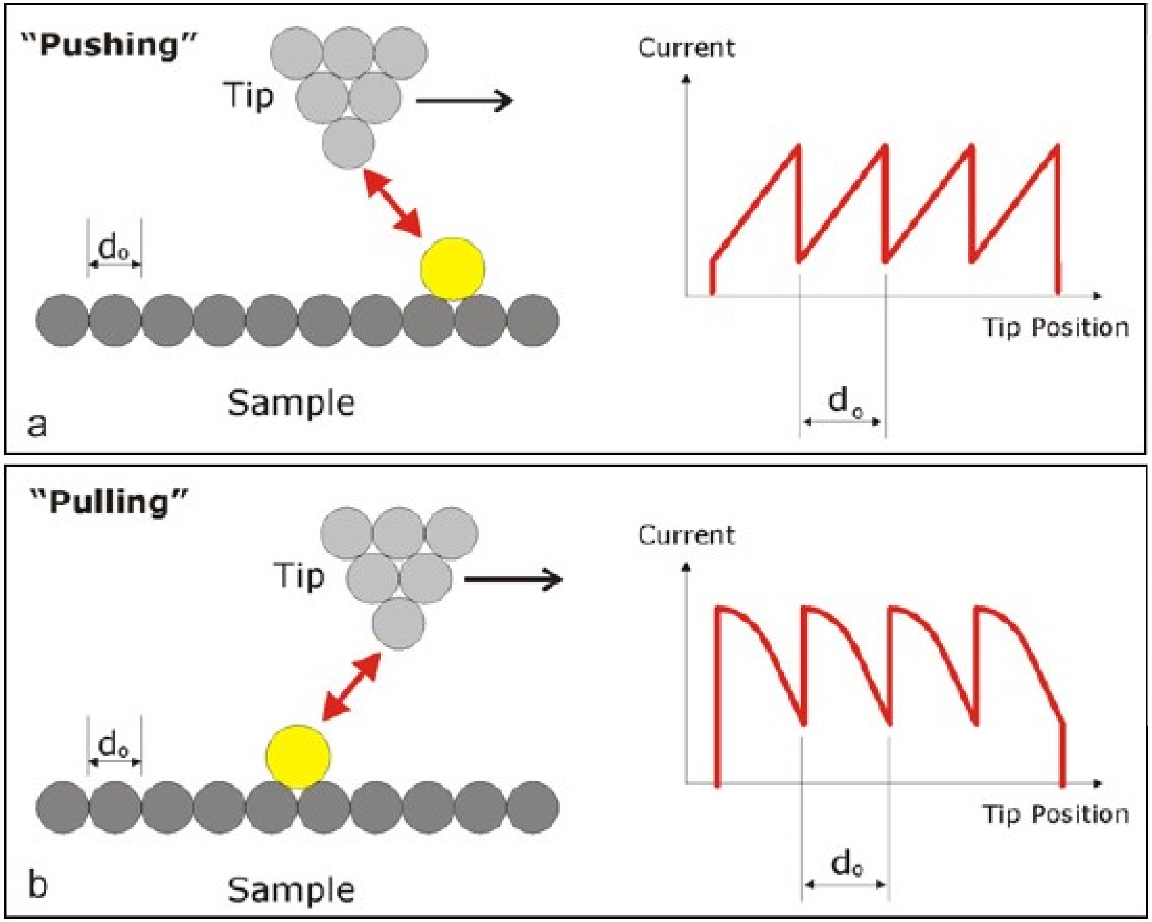

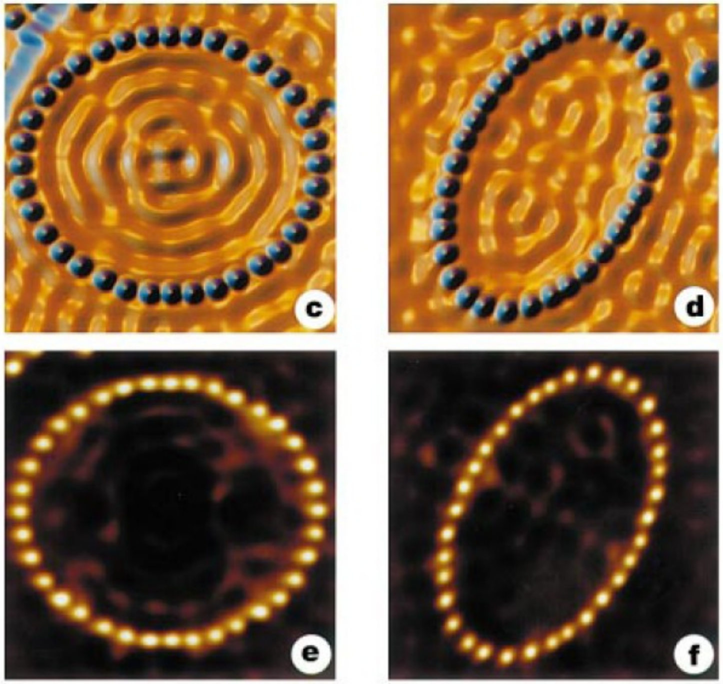

Cobalt on Cu(111)

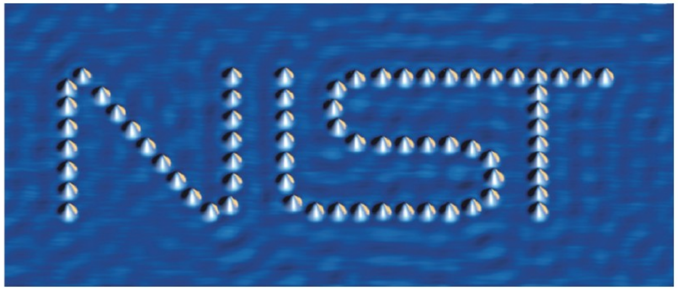

A 40-nm wide logo for NIST (National Institute of Standards and Technology), made by the manipulation of Co atoms on a Cu(111) surface

Magneto-transport measurements for TI

- Weak localization (WL) and weak anti-localization (WAL)are quantum interference effects in quantum transport in a disordered electron system.
- WAL enhances the conductivity and WL suppresses the conductivity with decreasing temperature at very low temperatures.
- A magnetic field can destroy the quantum interference effect, giving rise to a cusp-like positive and negative magnetoconductivity as the signatures of WL and WAL, respectively. These effects have been widely observed in topological insulators.

- **WAL:** an advantageous magneto-resistance (MR) effect, occurs as a result of suppression of TRS in the system when exposed to an external magnetic field.
- The WAL effect in pure TI thin films is characterized by cusp-like magnetoconductance data at low temperatures and near-zero magnetic fields. Cusp-like shape is highly dependent on the film thickness, and it is observed that the WAL effect is suppressed by the bulk conductance in relatively thicker films

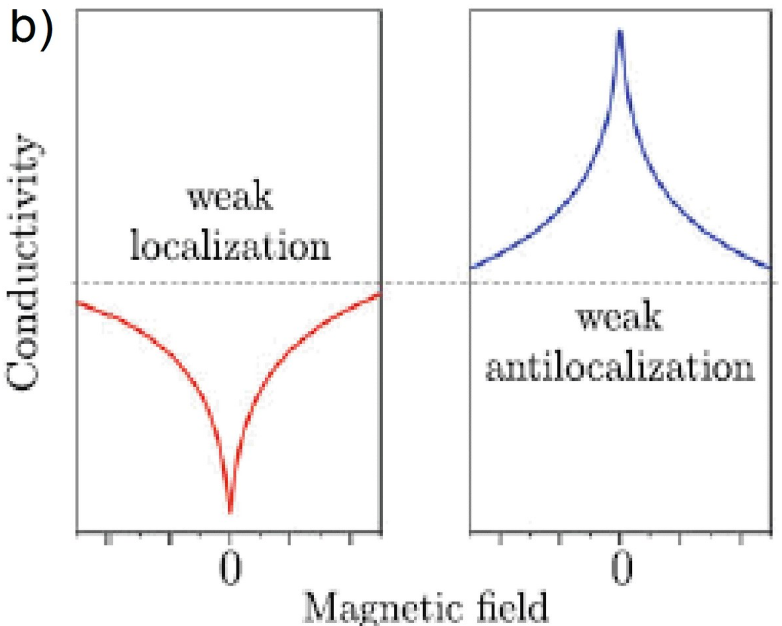

S.Q. Shen, Topological Insulators, Springer (2012)

Bi_2Se_3 TI thin films: Magnetron sputtering system

Magnetron sputtering system:

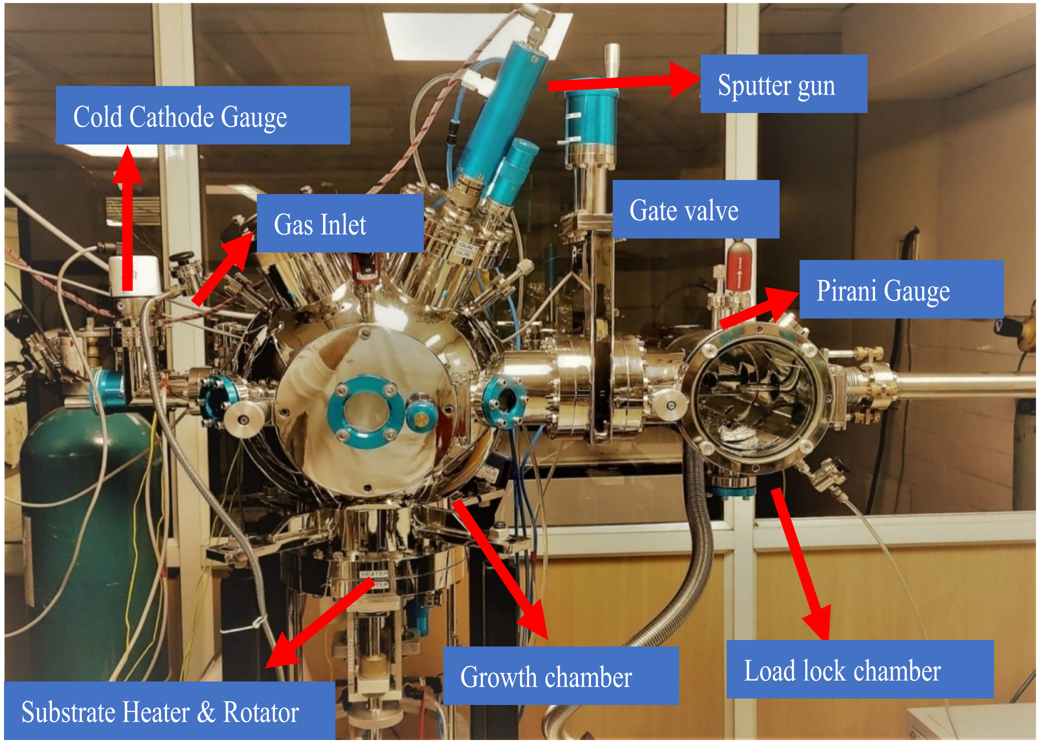

- Base Pressure < 2×10^{-7} mbar
- Substrate Heater: ≤ 1000 °C
- Bi_2Se_3 (Purity-99.99%) sputtering target
- Substrates: Molybdenum (Mo), Titanium (Ti) foil (Purity-99.95%)

Deposition parameters:

Temp: 350-450°C, RF Power: 10-20 W,
Ar flow rate: 10-20 sccm, Pressure: 3.3E-3 mbar.

Post-selenization process:

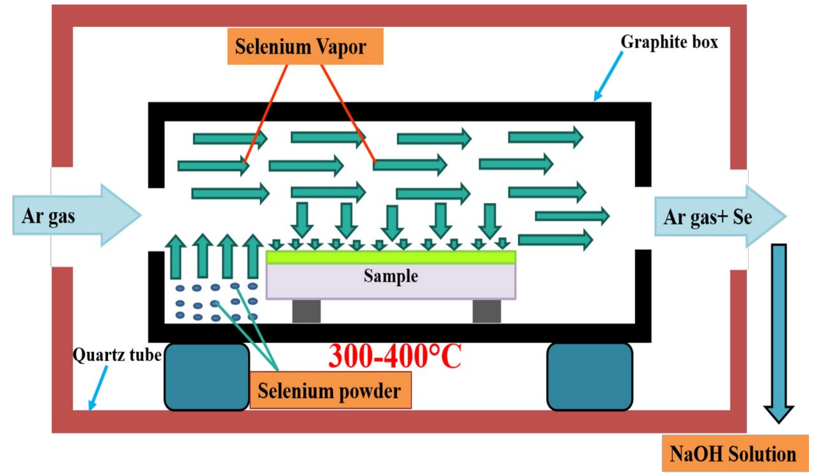

Post-Selenization process: Temperature at 300-400 °C in a furnace with Ar gas flow for 30-90 min.

Characterization

- Raman spectroscopy in backscattering mode
- XRD - Cu-$K_{\alpha 1}$ X- ray source (λ= 0.15406 nm)
- FESEM (15 kV operating voltage)
- XPS (Energy of AlK $_{\alpha}$ source: 1486.7 eV)

Bi_2Se_3 TI films on sapphire (0001) by magnetron sputtering

S1: 40 nm, S2: 80 nm and S3: 160 nm. Deposition rate and thickness calibrated by cross-sectional SEM and AFM.

HR-XRD

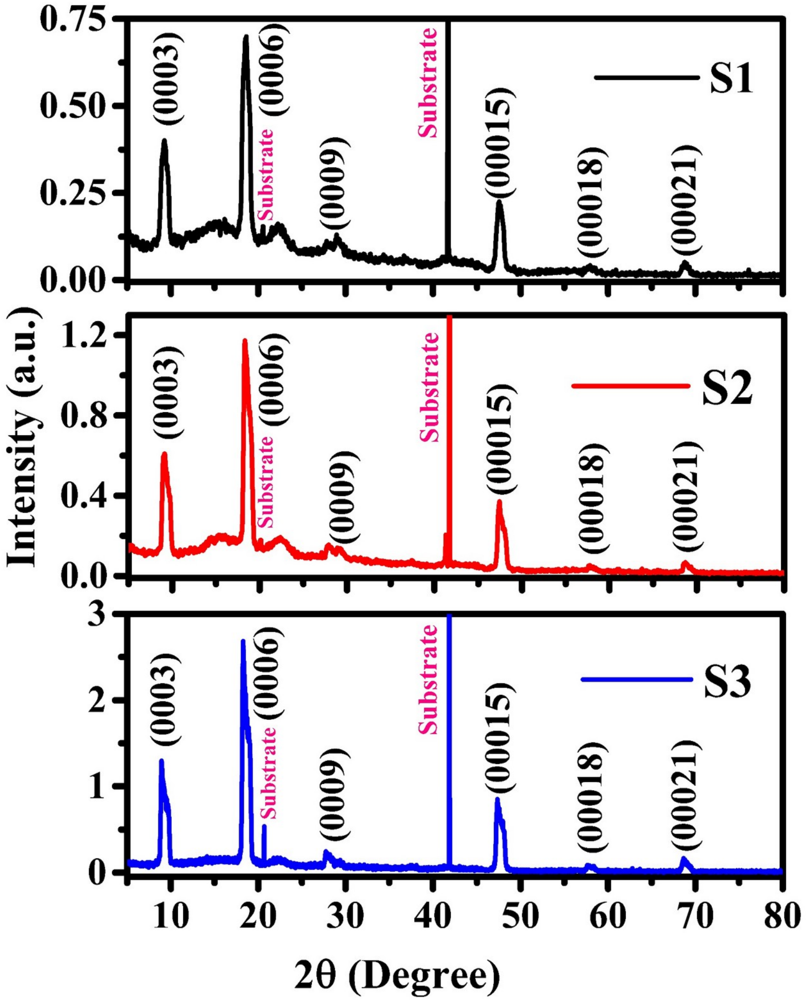

- The HR-XRD measurements revealed the growth of rhombohedral c-axis {0003n} oriented Bi_2Se_3 films on sapphire (0001).

Raman spectra

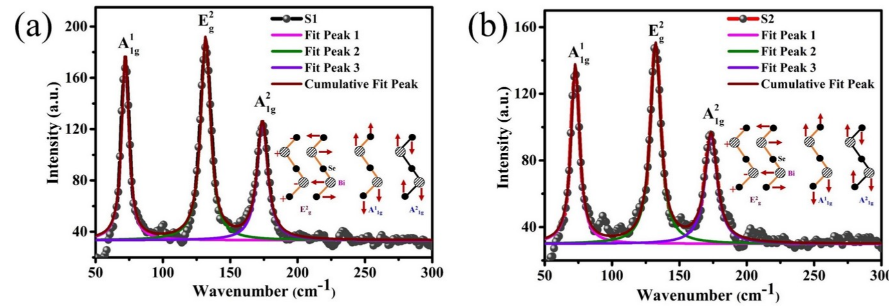

Vibrational modes of Bi_2Se_3 thin films were obtained in the low wave number region.

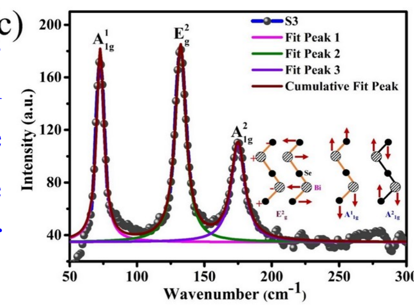

Three Raman peaks namely A^1_{1g}, E^2_g, and A^2_{1g} were detected in low wavenumber region for all samples (S1-S3).

Sample Name	A^1_{1g} Peak (cm^{-1})	A^1_{1g} FWHM (cm^{-1})	E^2_g Peak (cm^{-1})	E^2_g FWHM (cm^{-1})	A^2_{1g} Peak (cm^{-1})	A^2_{1g} FWHM (cm^{-1})
S1	72.11	6.43	131.73	8.71	173.87	9.59
S2	72.75	7.49	132.31	9.38	173.52	11.02

Surface morphology of Bi_2Se_3 TI films on sapphire (0001)

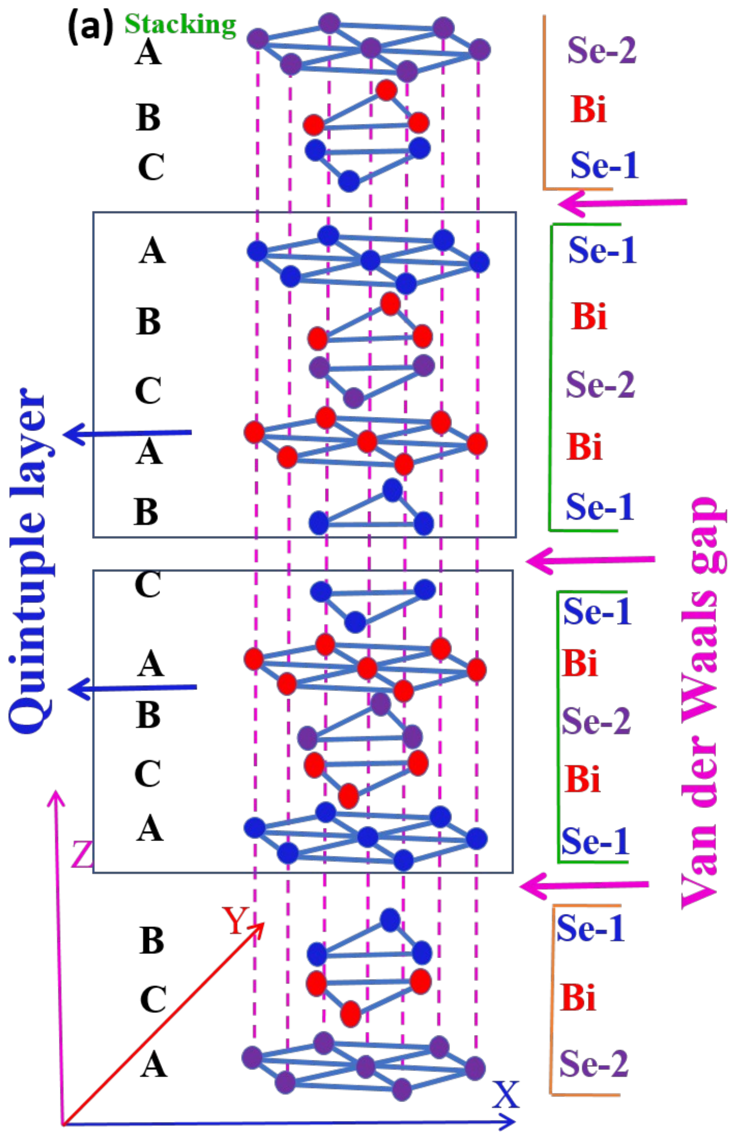

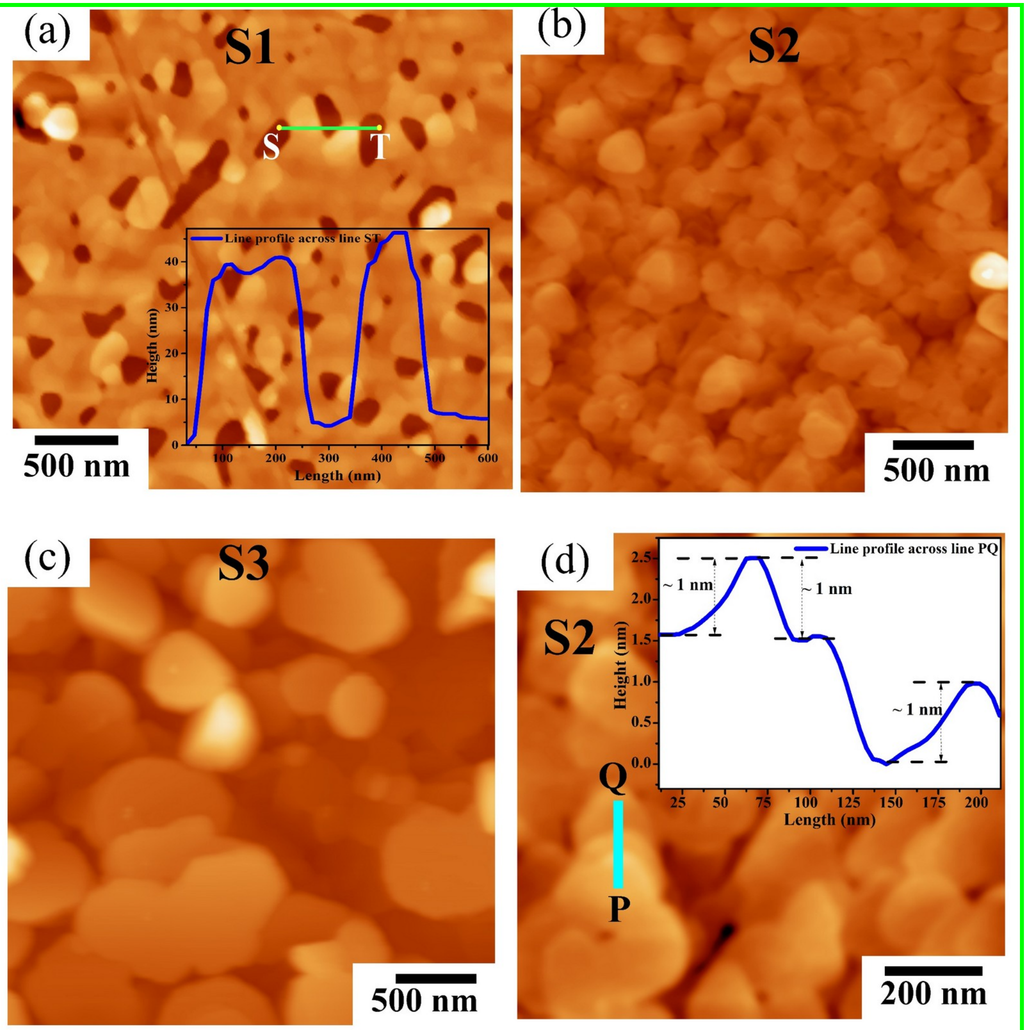

Tapping mode AFM images for samples S1 (a), S2 (b) and S3 (c). (d) AFM image of sample S2 with scan area of (1 μm)² and inset shows the line profile across PQ line, showed the growth of QL thickness. Inset of (a) shows the line profile along ST line.

Sudhanshu Gautam et al. Sci. Rep. 12 (2022) 9770

Magneto-transport properties of Bi_2Se_3 thin films on sapphire (0001)

R-T curves for S1-S3 samples

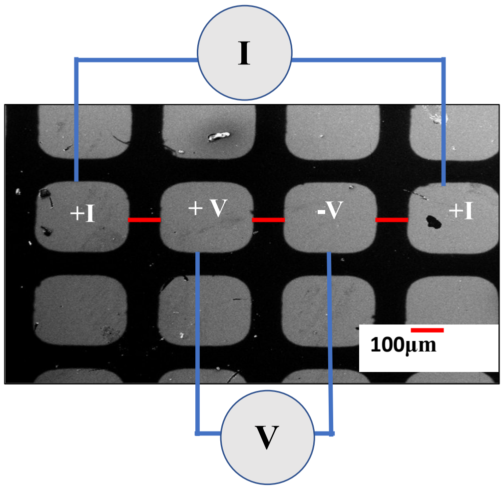

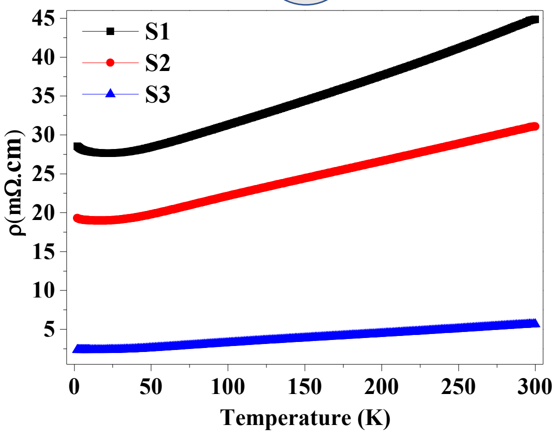

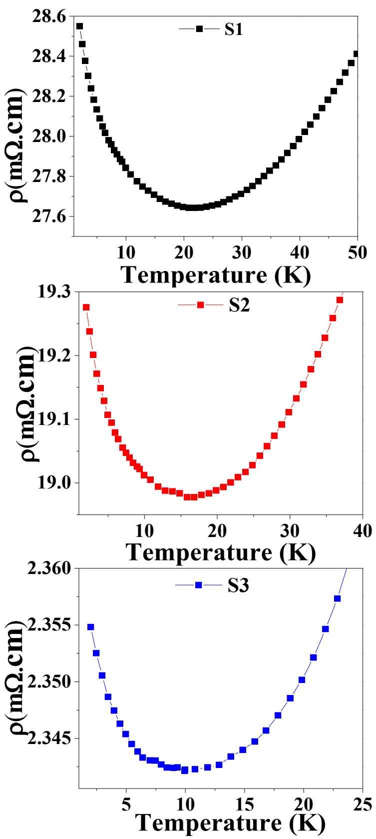

- Temperature-dependent resistivity for Bi_2Se_3 thin films shows the metallic nature of thin films.
- Upturn in resistivity occurred at 21 K, 16 K, and 11 K for 40 nm, 80 nm, and 160 nm film respectively.

$$MR\% = \frac{R(B)-R(0)}{R(0)} \times 100$$

Where, R (B) and R (0) are resistances of film at the applied field and zero magnetic field, respectively

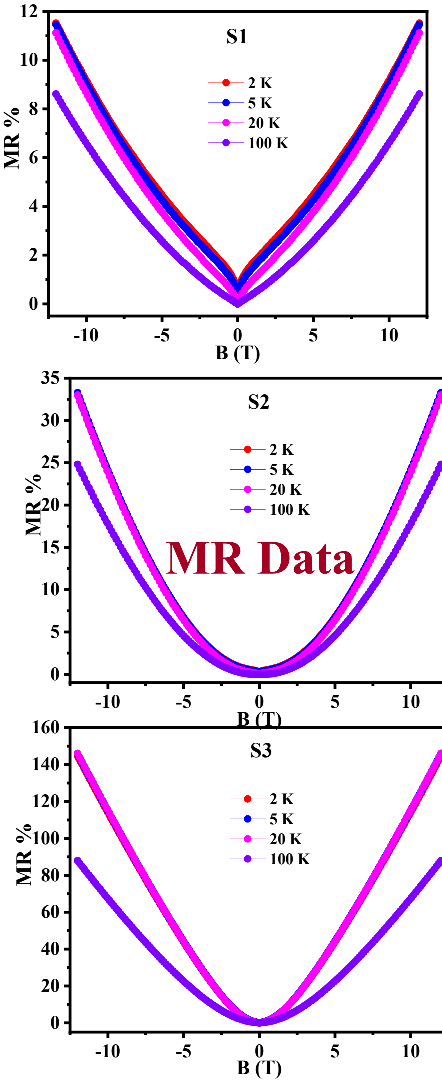

- MR curve depicts that the V-type shape takes a sharp change into a parabolic shape as the thickness increases.

Magneto-transport properties of Bi_2Se_3 thin films on sapphire (0001)

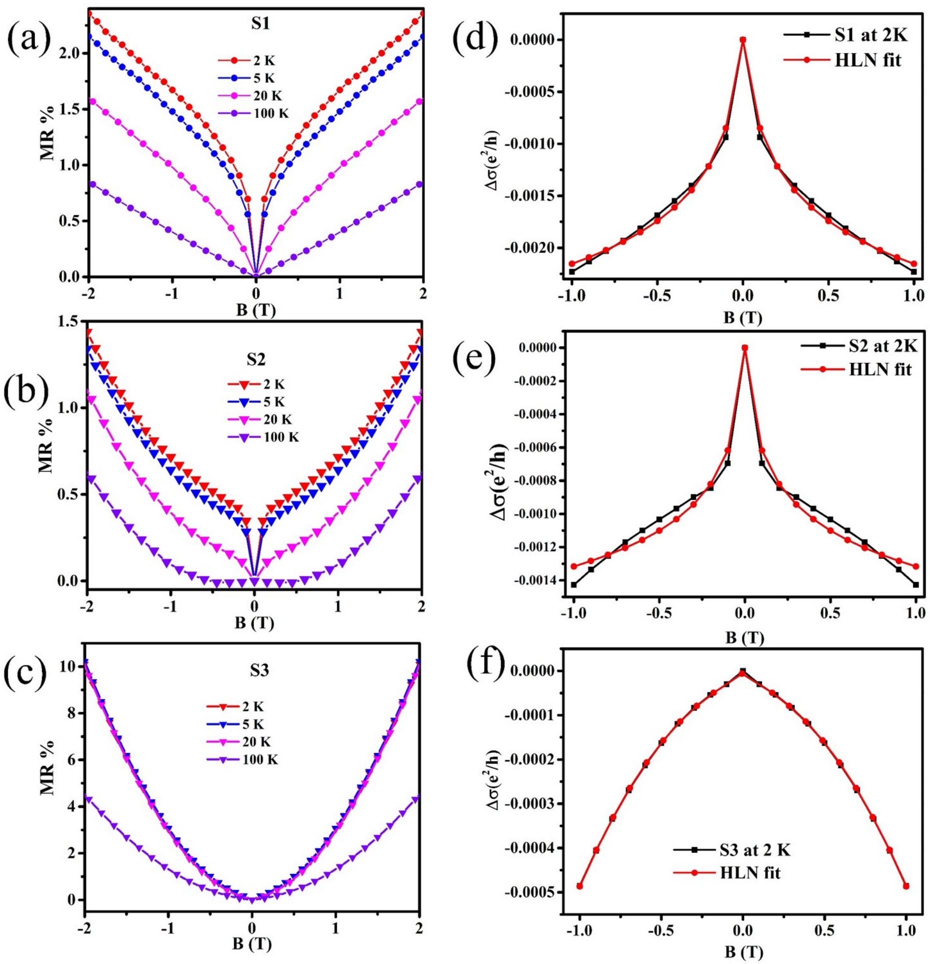

HLN model for magnetoconductivity fitting (S1 and S2):

$$\Delta\sigma(B) = -\frac{\alpha e^2}{2\pi^2 h}\left[ln\left(\frac{B_\Phi}{B}\right) - \Psi\left(\frac{1}{2} + \frac{B_\Phi}{B}\right)\right]$$

Where α indicates the total number of independent conducting channels, $B_\Phi = \frac{\hbar}{4eL_\Phi^2}$ is the characteristic field, L_Φ is the effective dephasing length and Ψ digamma function.

Modified HLN model for magnetoconductivity fitting (S3):

$$\Delta\sigma(B) = -\frac{\alpha e^2}{2\pi^2 \hbar}\left[ln\left(\frac{B_\Phi}{B}\right) - \Psi\left(\frac{1}{2} + \frac{B_\Phi}{B}\right)\right] + \lambda B$$

Where λ is a linear term that is taken into account to reduce the effect of classical linear MR

- **An ideal TI is expected to have an α value of 1.**
- **Some reported values of α are found in the range of -0.50 to 0.50 also.**

The quantum correction to the magnetoconductivity of thin films in low magnetic field is done by employing Hikami- Larkin- Nagaoka theory and the calculated value of coefficient 'α' (defining number of conduction channels) was found to be 0.65, 0.83 and 1.56 for film thickness of 40, 80 and 160 nm, respectively.

M. Liu et al. Phys. Rev. Lett. 108 (2012) 036805

L. J. C. McIntyre et al.EPL, 107 (2014) 57009.

W. J. Wang et al. Scientific Reports 6 (2016) 25291

S. Gautam et al. Scientific Reports 12 (2022) 9770

TI for QHE Application

- **The existence of a 2D topologically insulating state was predicted by Kane et al. [PRL 95 (2005) 226801] and the first 2D TI material (HgTe/CdTe quantum wells) was predicted by Zhang et al. [Science 314 (2006) 1757].**
- The chalcogenides Bi_2Se_3, Bi_2Te_3 are model examples of 3D TIs as these materials possess the single Dirac-like band in topological surface state. [Zhang et al. Nature Physics 5 (2009) 438]
- **Bi_2Se_3 has been studied extensively due to larger band gap (~ 0.3 eV) compared to Bi_2Te_3 (~0.1 eV), offering more control at elevated temperature.**

QHE observation in un-doped Bi_2Se_3 film

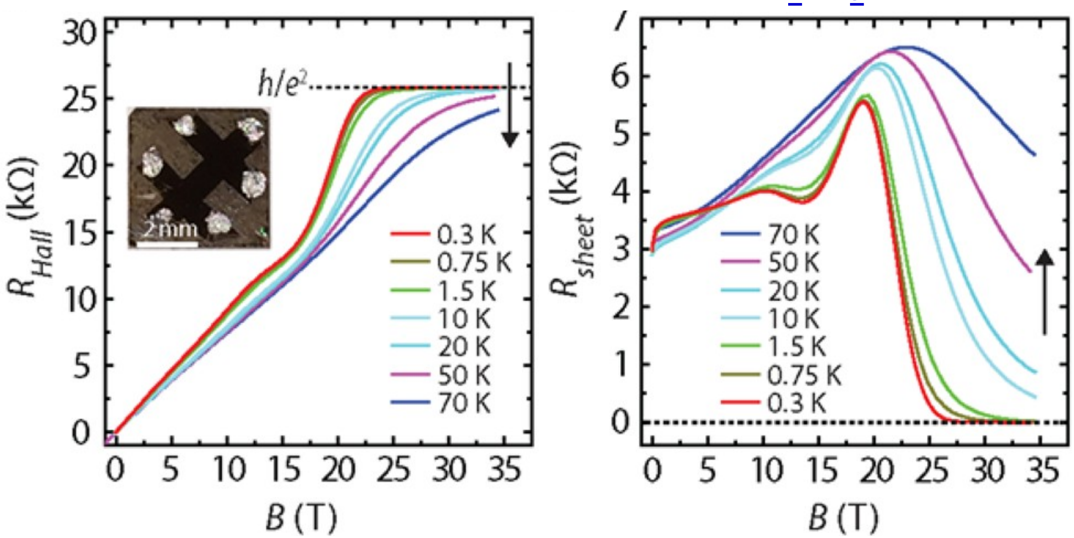

❑The data for 0.3 K shows that R_{sheet} vanishes (0.0 ± 0.5 Ω) above 31 T indicating dissipation less transport with simultaneous perfect quantization of R_{Hall} = (1.00000 ± 0.00004)h/e2 (25813 ± 1 Ω) above **29 T**: **Need high magnetic field**

N. Koirala et al. Nano Lett. 15 (2015) 8245−8249

Magnetic doped TIs

❖ One of the most promising ways to break TRS is based on the magnetically doped TIs where the interplay of strong-orbit coupling and magnetic exchange interaction promotes the band inversion.

❖Breaking TRS of a Bi_2Se_3 TI thin film by magnetic doping opens up a mini-gap of the Dirac surface state and it is expected to play important role in field of quantum anomalous Hall effect (QAHE).

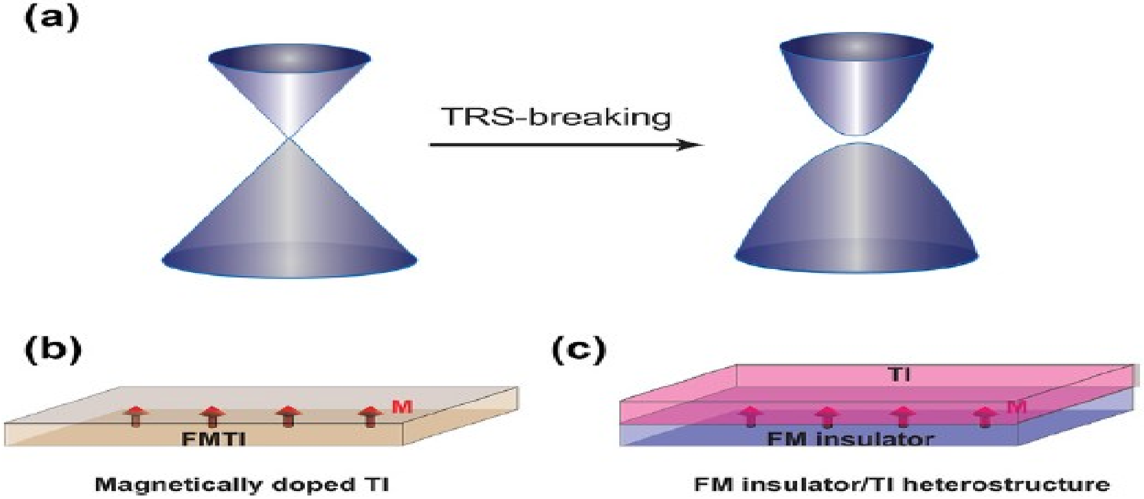

Time-reversal symmetry (TRS)-breaking of TI. (a) Surface states diagram in TI and TRS-breaking TI. (b) Magnetically doped TI film (c) a FM insulator/TI heterostructure.

➢ The high quality un-doped bulk single crystals of TIs are preferred to study quantum oscillations by electrical transport. However, the bulk defects and natural doping in Bi_2Se_3 due to the presence of Se-vacancies lead to a contribution of the bulk carrier density to the conductivity.

➢ Therefore, for investigations of the surface states, fabrication of thin films and layers of TIs is preferred.

Magnetic TI for QAHE Application

AQHE observation in Mn-doped Bi_2Te_3 film

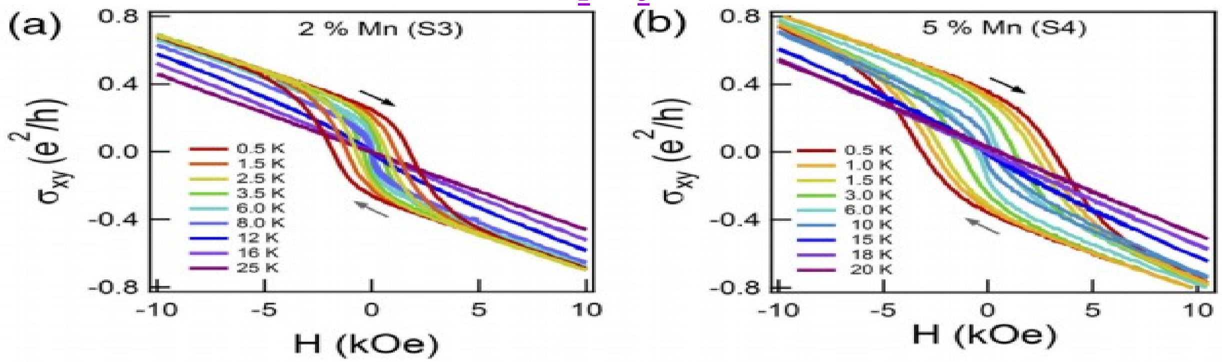

(a-b) Temperature dependence of the Hall conductivity σ_{xy} for Mn-doped bismuth telluride films with 2% Mn , 5% Mn respectively

J. S. Lee et al. Phys. Rev. B 89, 174425 (2014)

AQHE observation in Cr-doped Bi_2Te_3 film

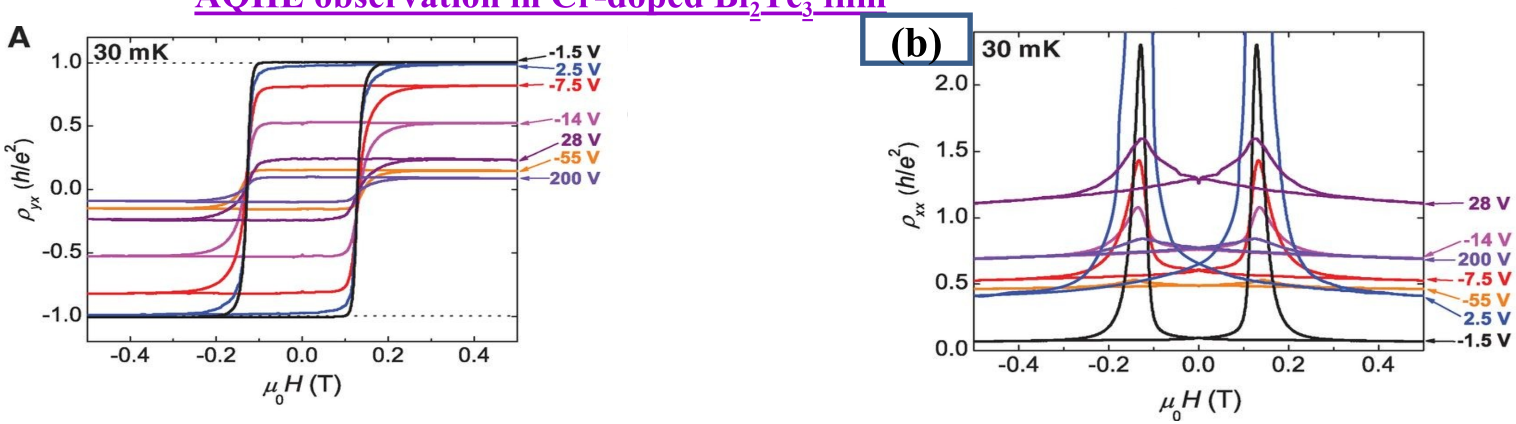

- ❑ At zero magnetic field, the gate tuned anomalous Hall resistance reaches the predicted quantized value of *h/e2*, with considerable drop of the longitudinal resistance.

C. Z. Chang et al. Science 340 (2013) 167

Magnetic TI for QAHE Application

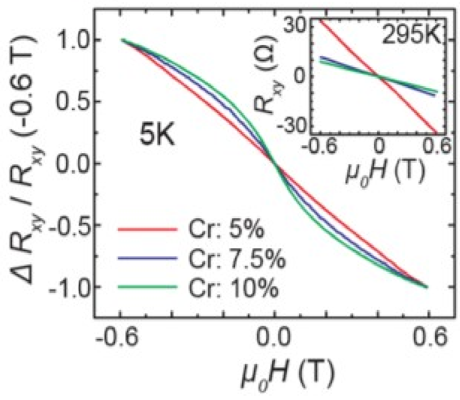

Ferromagnetic **Anomalous Hall Effect** in **Cr-Doped Bi_2Se_3 Thin Films** via Surface-State Engineering

Moon et al. Nano Lett. 2019, 19, 3409

- Precision measurement of the quantized anomalous Hall resistance at zero magnetic field in **V-doped $(Bi,Sb)_2Te_3$** thin films

Gotz et al. Appl. Phys. Lett. 112 (2018) 072102

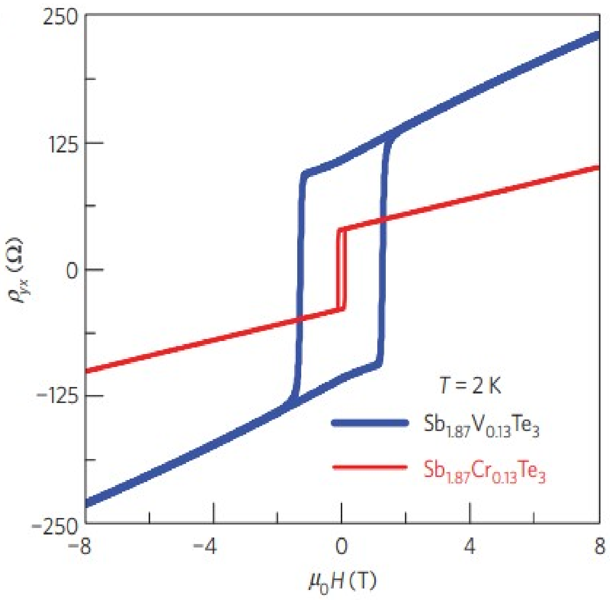

Comparison of the hall traces in Cr- and V-doped Sb_2Te_3.

V-doped system is clearly a more precise experimental confirmation of the ideal QAH effect than that in the Cr-doped system.

C. Z. Chang et al. Nat. Mater. 473–477(2015)

- **The realization of the QAHE effect may lead to the development of low-power-consumption electronics.**

Cr-doped of Bi_2Se_3 thin films on STO (100) and (110) substrates

HRXRD

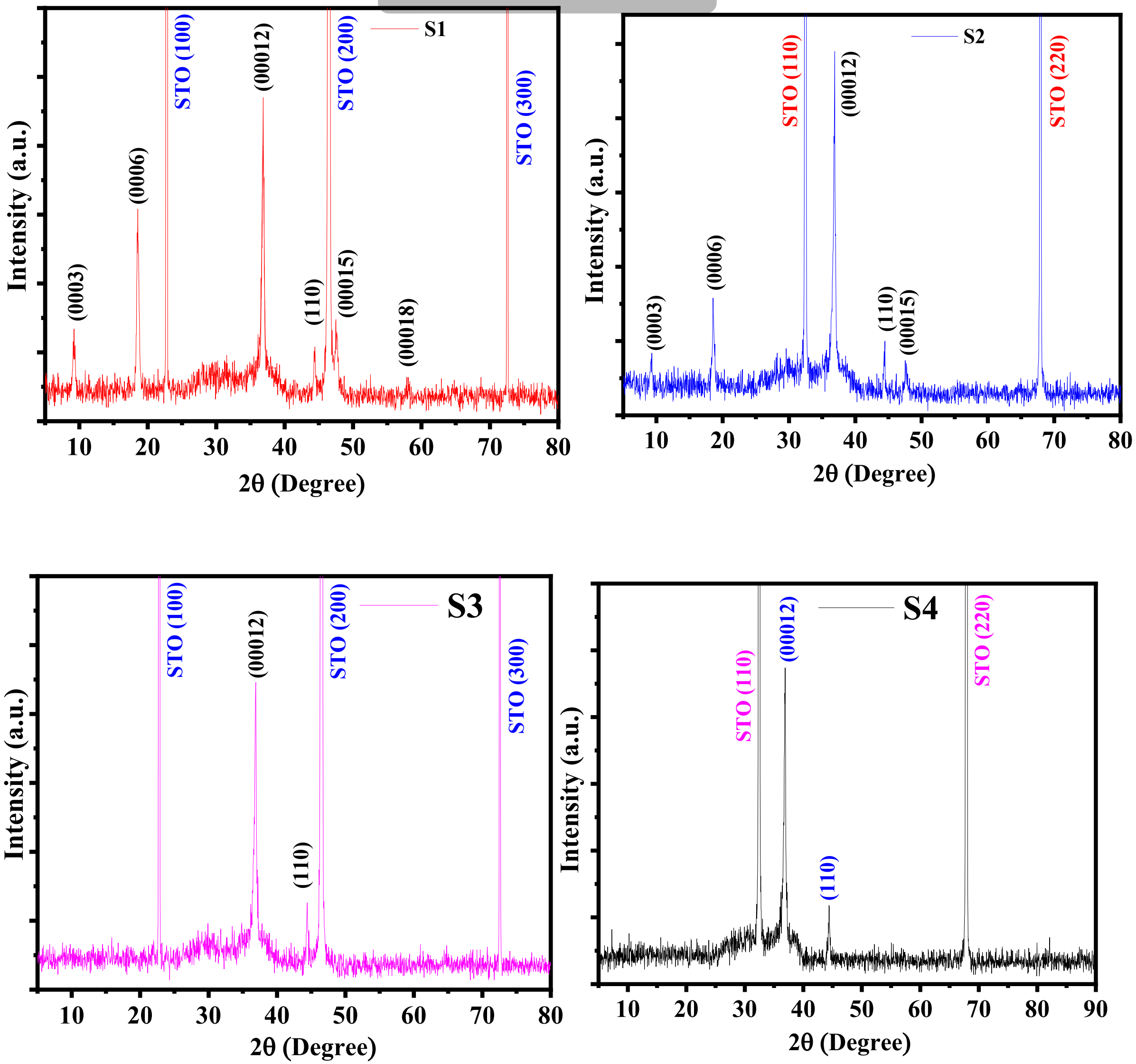

- ❖ HR-XRD revealed the growth of our Bi_2Se_3 thin film is highly oriented along the C-axis.
- ❖ Most of the peaks correspond to the (0003n) hexagonal plane on both substrates except the (110) peak.
- ❖ In Cr-doped samples other {0003n} planes are not visible except the (00012) plane.
- ❖ It is likely due to the Cr starts to replace Bi.

Cr-doped of Bi_2Se_3 thin films on STO (100) and (110) substrates

Rutherford backscattering (RBS)

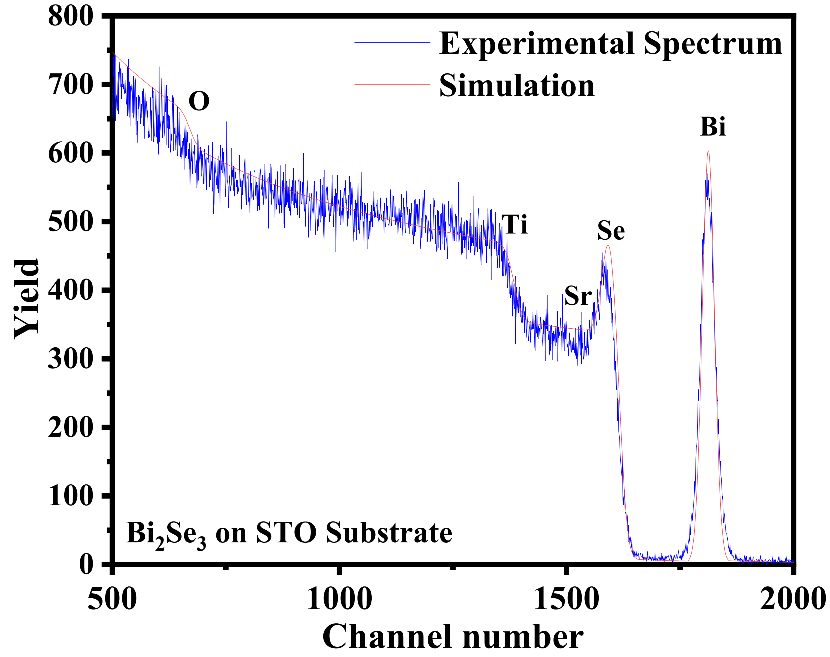

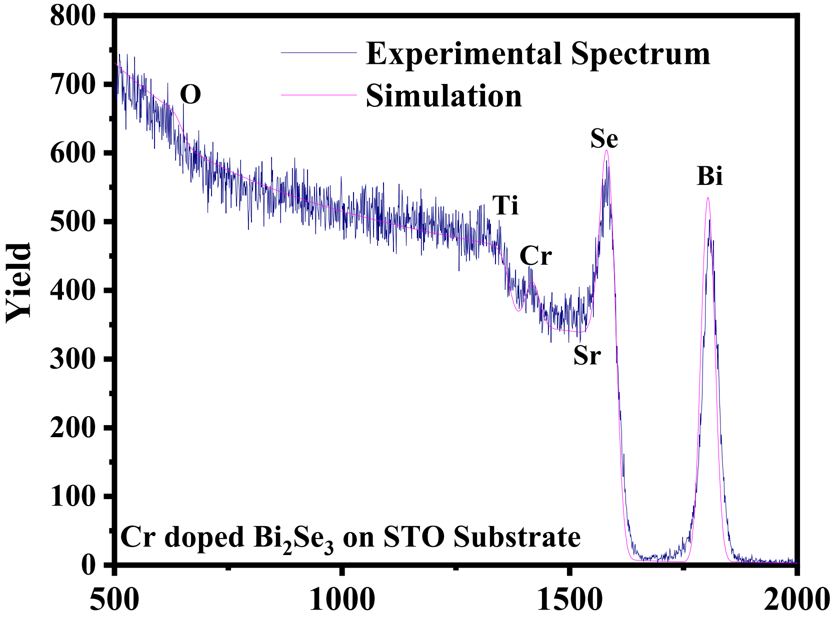

- The RBS measurements were performed using a 5SDH-1.7MV Tandem accelerator The energy of the well-collimated He^{++} ion beam used is 2 MeV
- RBS data revealed that the Cr replaced Bi in the magnetic doped Bi_2Se_3, and Cr dopant in the Bi_2Se_3 turned out to be ~ 0.18.

Cr-doped of Bi_2Se_3 thin films on STO (100) and (110) substrates

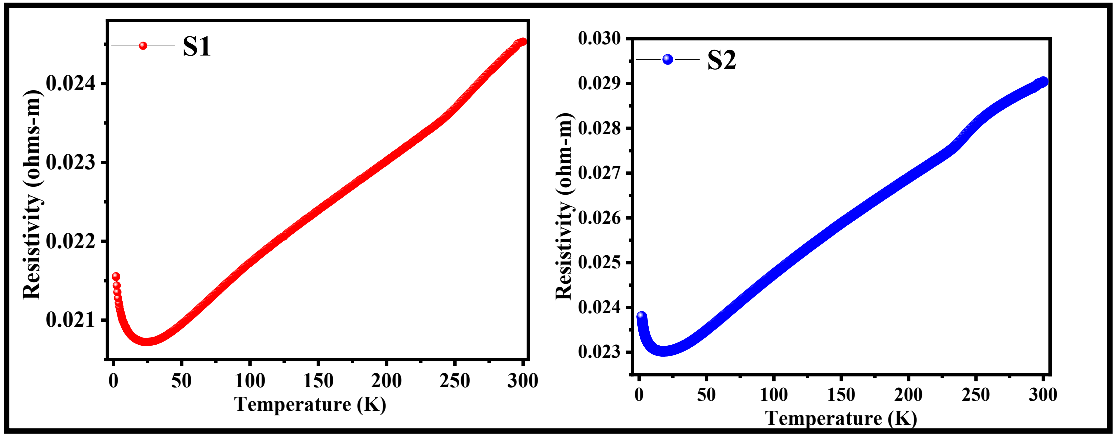

- In samples S1 and S2 resistivity monotonically decreases with decreasing temperature and shows strong metallic behavior.
- After reaching temperature ~30 K resistivity takes a slight upturn.

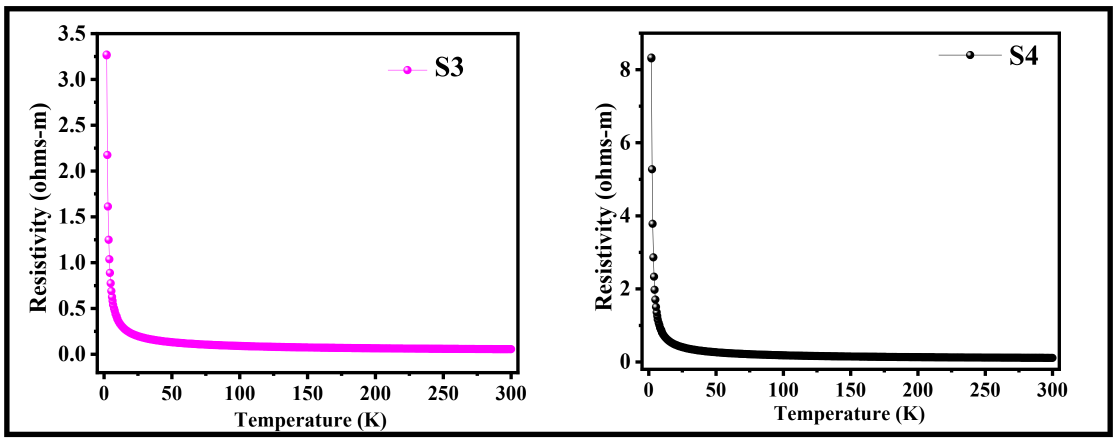

- Samples S3 and S4, with Cr doping, the monotonic increase in resistivity as the temperature decreases, reveals typical semiconductor characteristics

X. F. Kou et al. Journal of Applied Physics, 112 (2012) 063912

M. Liu et al. Phys. Rev. Lett. 108 (2012) 036805.

Cr-doped of Bi_2Se_3 thin films on STO (100) and (110) substrates

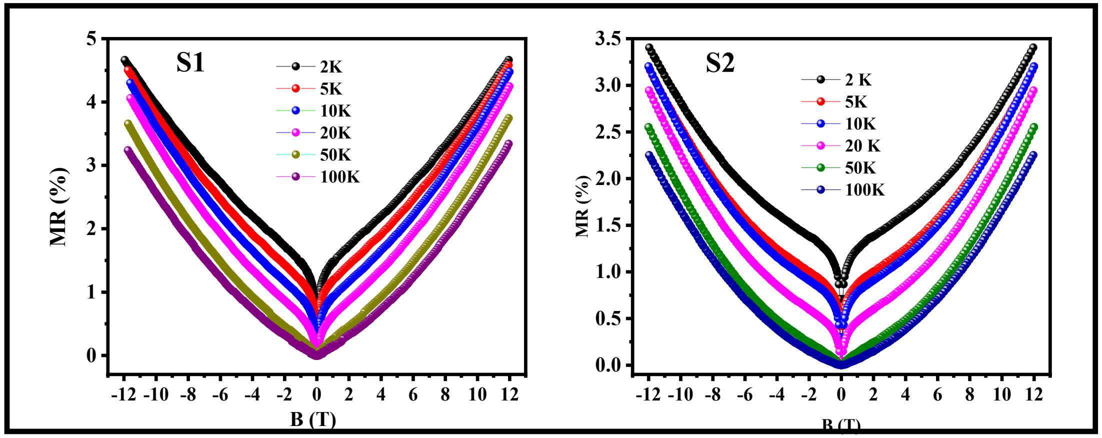

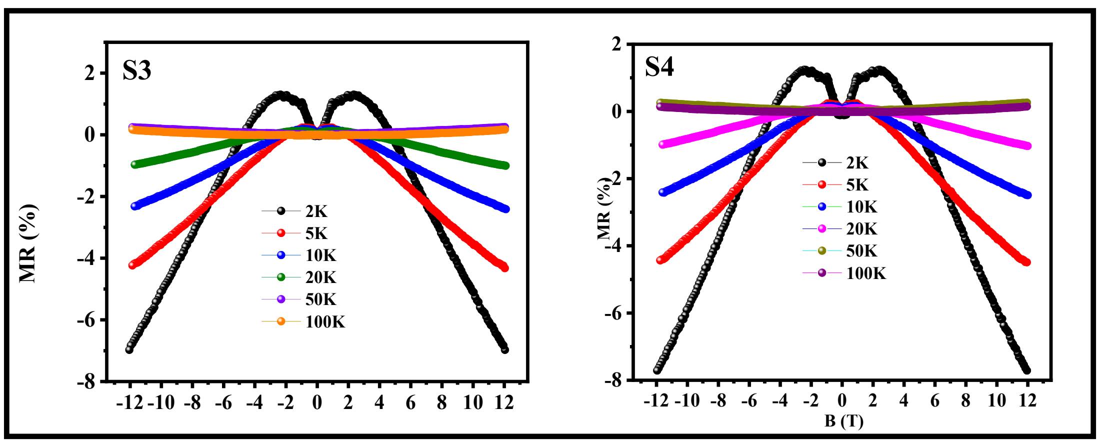

- **MR data of samples S1 and S2 shows a positive cusp-like shape which is a characteristic feature of quantum effect WAL in TIs. At low temperatures (2-20 K), cusp is found to be very prominent.**
- **The cusp-like MR data started to take a parabolic shape and at 50 K and 100 K, this WAL feature vanished.**

- **MR data of samples S3 and S4 shows Positive magnetoresistance with a sharp cusp up to 20K in the short magnetic field range (-2T to 2T) is visible**
- **At higher magnetic fields, a negative magnetoresistance can be seen and vanished at temperature 50K, which describes the WL effect**

Sudhanshu Gautam et al. J. Appl. Phys. 135 (2024) 19441

MTI based QAHE for QHRS

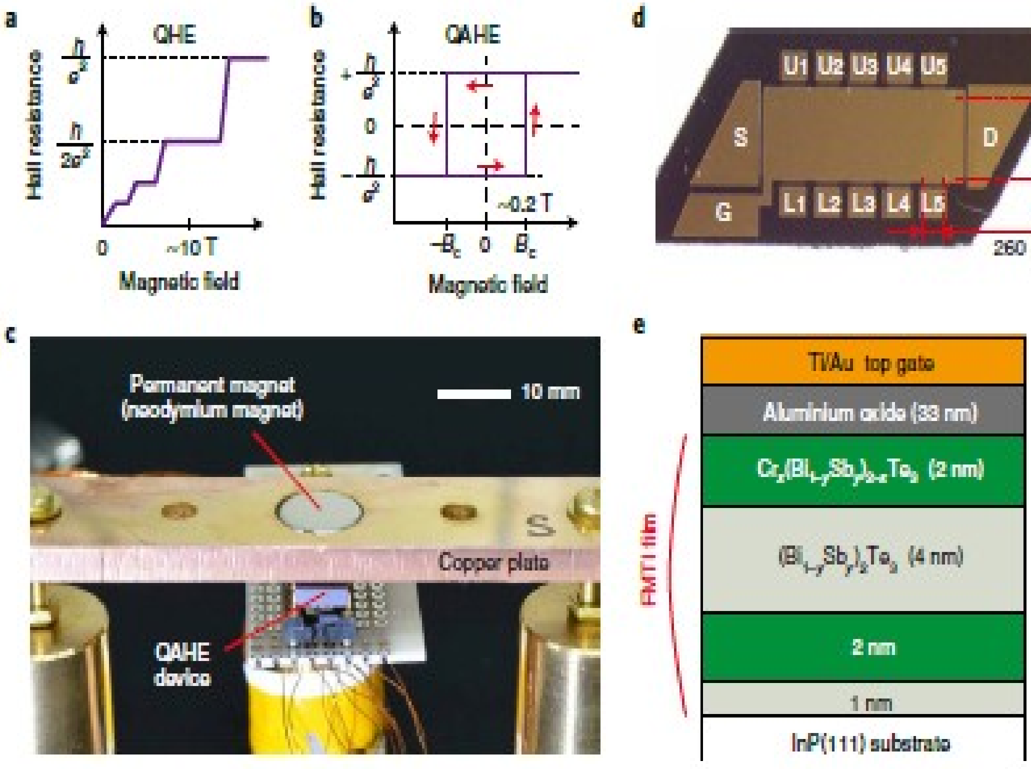

Schematic of magnetic field dependant on QHE and QAHE devices. Small permanent magnet is sufficient to produce quantized Hall resistance with a precision of 10 parts per billion.

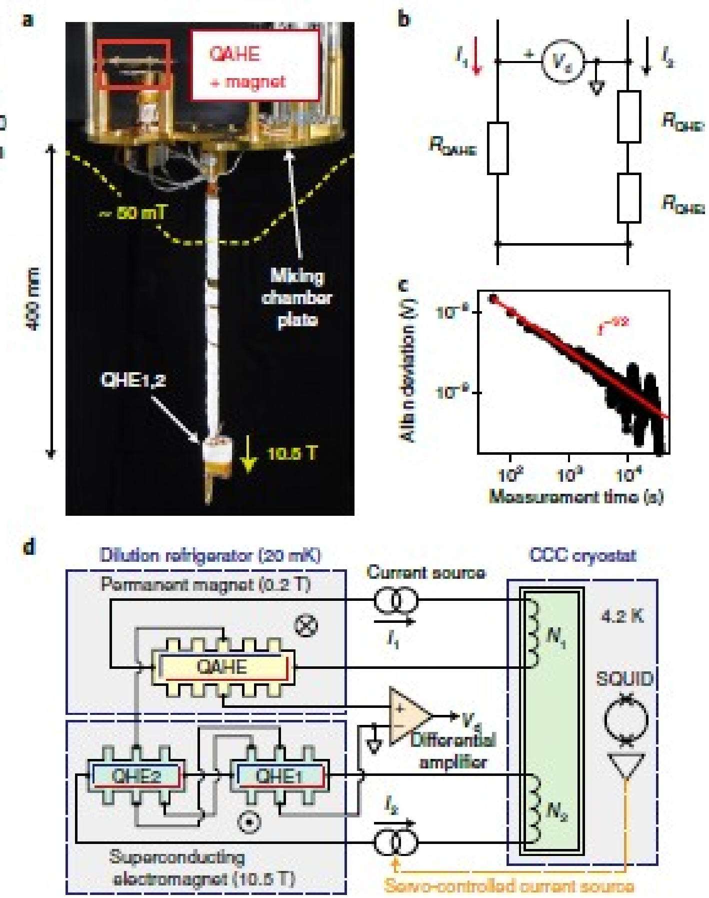

Direct comparison with QHE in strong magnetic field and QAHE in small permanent magnet.

Okazaki et al. Nat. Phys. 18, 25 (2022)

QAHE using MTI: Current status

Current status of the precision measurements using AQHE in MTI devices

(MBE grown Cr/V($Bi_{1-x}Sb_x$)Te_3 films/heterostructures)

(***$\delta\rho_{xy}$***: the deviation of the Hall resistivity from quantization and ***ρ_{xx}*** : the lowest reported longitudinal resistivity).

NMIs	$\delta\rho_{xy}$	ρ_{xx}	Current	Ref.
NIST-Stanford (2018)	0.04 μΩ/Ω ± 0.26 μΩ/Ω	1.9 mΩ ± 6.2 mΩ	≤ 10 nA	Phys. Rev. B 98, 075145 (2018)
PTB-UW (2018)	0.17 μΩ/Ω ± 0.25 μΩ/Ω	47.2 mΩ ± 12.9 mΩ	≤ 25 nA	Appl. Phys. Lett. 112, 072102 (2018)
NMIJ- Others (2020)	−1.7 μΩ/Ω ± 1.5 μΩ/Ω	3.5 Ω ± 1Ω	≤ 50 nA	Appl. Phys. Lett. 116, 143101 (2020)
NMIJ- Others (2022)	0.004 μΩ/Ω ± 0.01 μΩ/Ω	6 mΩ	~ 1 μA	Nat. Phys. 18, 25 (2022)
NIST-Stanford (2023)	−0.02 μΩ/Ω ± 0.31 μΩ/Ω	7.34 mΩ ± 1.60 mΩ	≤ 50 nA	Phys. Rev. Appl. 18, 034008 (2023)

MTI-based QAHE is presently limited to much lower (~50-100 nA) device currents compared to QHE (~50 – 500 μA), resulting in inferior measurement uncertainties

Quantum current: possible ways

The ampere, symbol A, is the SI unit of electric current. It is defined by taking the fixed numerical value of the elementary charge e to be 1.602 176 634 × 10–19 when expressed in the unit C, which is equal to A s, where the second is defined in terms of ∆ν Cs.

Practical realization of the ampere (Recommended by BIPM w.e.f. April 2019 onwards)

(a)by using Ohm's law, the unit relation A = V/Ω, and using practical realizations of the SI derived units the volt V and the ohm Ω, based on the Josephson and quantum Hall effects, respectively,

(b) by using a single electron transport (SET) or similar device, the unit relation A = C/s, the value of e given in the definition of the ampere and a practical realization of the SI base unit the second s; or

(c) by using the relation I = C·dU/dt, the unit relation A = F·V/s, and practical realizations of the SI derived units the volt V and the farad F and of the SI base unit second s.

Single electron transport (SET) implementations still have technical limitations and often larger relative uncertainties than some other competitive techniques. However, SET implementations are included in this Mise en pratique because they offer unique and elegant approaches to realizing SI units, and their uncertainties have been improving in recent years, and they promise to improve further in the future.

Quantum current: possible ways

A current standard based on QPS

Coherent quantum phase slips convert a microwave photon into a current that is proportional to the photon's frequency, thus, an accurate knowledge of the frequency translates to a precisely known current

Proposed Device Geometry

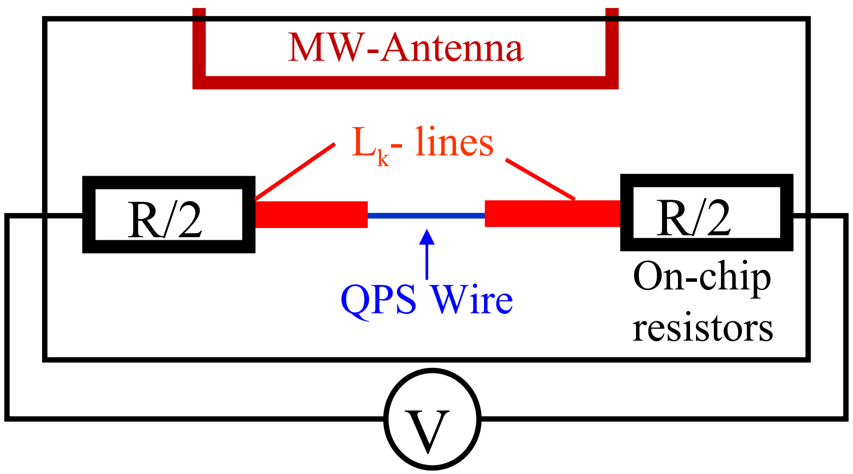

Proposed Materials:

1. Nb
2. NbGd
3. TiN
4. NbSi
5. Nb_xN

Shapiro steps at constant current in a QPS junction

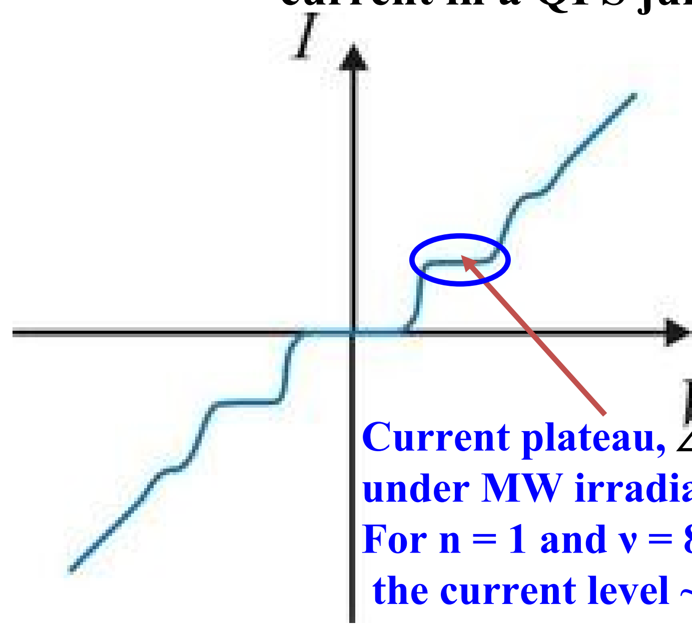

NbSi, CrO_2 can be used for on-chip resistive and inductive couplings

Mooij, Nazarov. *Nature Physics* 2, 169-172 (2006)

Quantum Phase Slip and transport

Superconducting TiN thin films featuring phase slip events

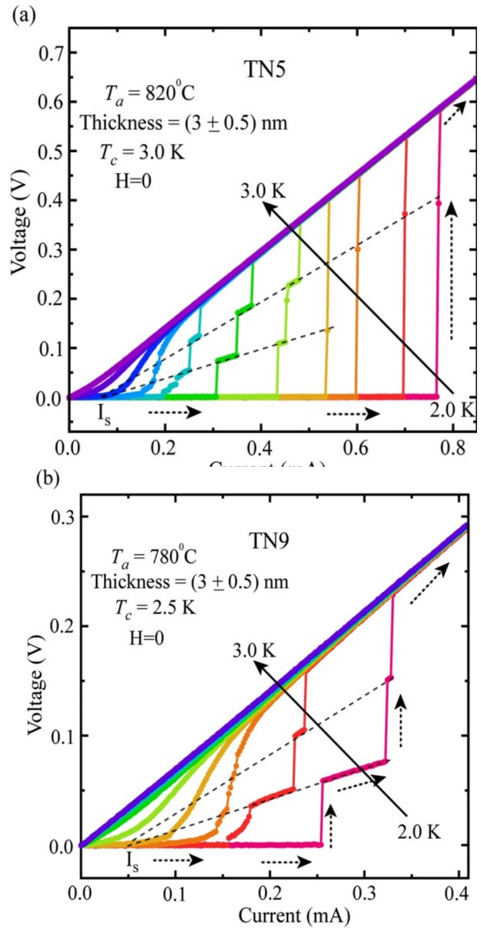

Zero-field IVC isotherms for (**a**) TN5 (~3 nm) annealed at 820 °C and (**b**) TN9 (~3 nm) annealed at 780 °C. Here, the samples TN5 and TN9 are of same thickness of about 3 nm. The dotted black arrows indicate the sweeping direction. The grey dashed lines indicate the convergence of the resistive states at the excess current I_s

S. Yadav et al. Sci. Rep. 11 (2021) 7888

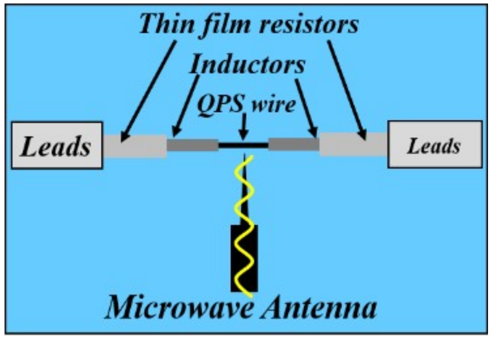

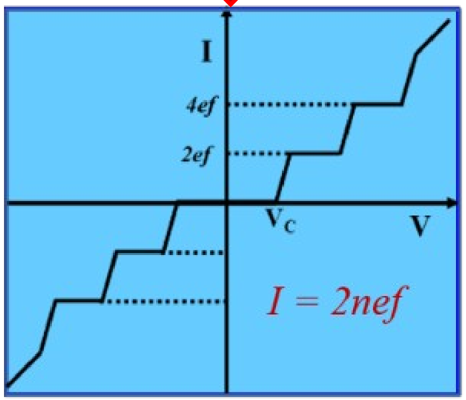

Substrate mediated nitridation of niobium into superconducting Nb_2N thin films for phase slip study

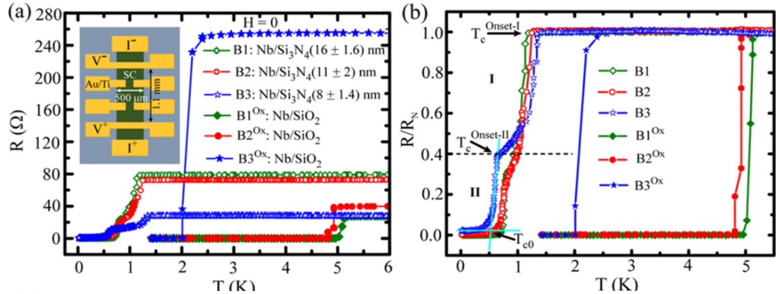

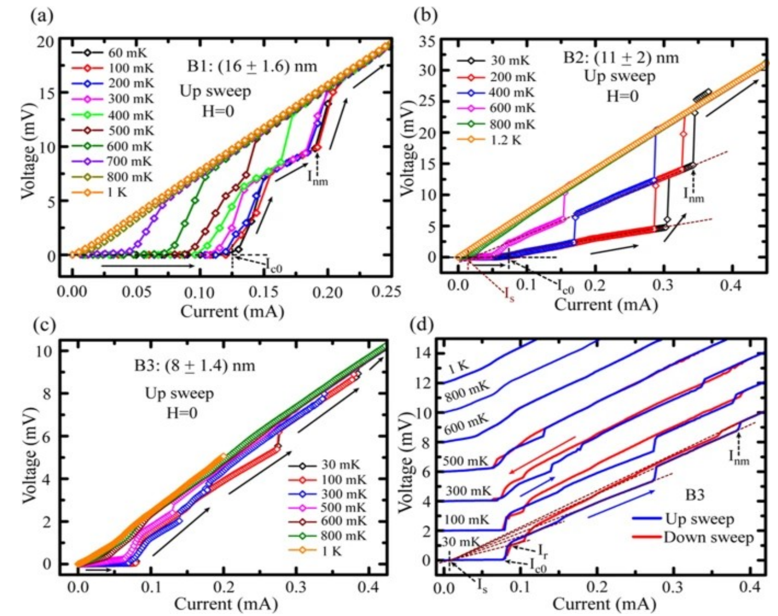

Current-voltage characteristics (*IVCs*) of Nb/Si_3N_4 samples measured under zero-field condition.

B. Gajar et al. Sci. Rep. 11 (2021) 7888

The Quantum Ecosystem

[BIPM]

Summary

- Metrology: **Once measured, accepted everywhere.**
- **Quantum Metrology**: **Utilizes quantum mechanics to enhance the precision and sensitivity of measurements beyond classical methods.**
- **Quantum materials**: **Exhibit properties not seen in classical physics, such as superconductivity, topological insulation, and quantum spin liquids.**
- Quantum based characterization techniques like STM: **powerful technique to see atoms at nanoscale**.
- Application of quantum materials: **QAHE devices, QPS and other quantum devices towards quantum metrology.**

Acknowledgements

- Director, CSIR-NPL
- Prof. Wang Xue-Sen, NUS Singapore
- Head Div #2 and Head DP#2.05, CSIR-NPL
- Dr. D. D. Shivagan and Dr. S. Panja
- Dr. Sudhanshu, Dr. Vishnu, Mr. Bheem, Mr. Rahul
- Surface Science and PLD Lab members
- SERB-DST and CSIR-NPL funding

Thank you